Bicyclic-Capped Histone Deacetylase 6 Inhibitors with Improved Activity in a Model of Axonal Charcot−Marie−Tooth Disease

Sida Shen,[†,∥] Veronick Benoy,[‡,∥] Joel A. Bergman,[†,∥] Jay H. Kalin,[†] Mariana Frojuello,[†] Giulio Vistoli,[§] Wanda Haeck,[‡] Ludo Van Den Bosch,[*,‡] and Alan P. Kozikowski[*,†]

[†]Drug Discovery Program, University of Illinois at Chicago, 833 S. Wood St., Chicago, Illinois 60612, United States
[‡]Laboratory of Neurobiology, Vesalius Research Center (VIB) and Leuven Research Institute for Neuroscience and Disease (LIND), KU Leuven, O&N4 Herestraat 49, B-3000 Leuven, Belgium
[§]Dipartimento di Scienze Farmaceutiche, Università degli Studi di Milano, Via Mangiagalli 25, 20133 Milano, Italy

Ⓢ Supporting Information

ABSTRACT: Charcot−Marie−Tooth (CMT) disease is a disorder of the peripheral nervous system where progressive degeneration of motor and sensory nerves leads to motor problems and sensory loss and for which no pharmacological treatment is available. Recently, it has been shown in a model for the axonal form of CMT that histone deacetylase 6 (HDAC6) can serve as a target for the development of a pharmacological therapy. Therefore, we aimed at developing new selective and activity-specific HDAC6 inhibitors with improved biochemical properties. By utilizing a bicyclic cap as the structural scaffold from which to build upon, we developed several analogues that showed improved potency compared to tubastatin A while maintaining excellent selectivity compared to HDAC1. Further screening in N2a cells examining both the acetylation of α-tubulin and histones narrowed

down the library of compounds to three potent and selective HDAC6 inhibitors. In mutant HSPB1-expressing DRG neurons, serving as an in vitro model for CMT2, these inhibitors were able to restore the mitochondrial axonal transport deficits. Combining structure-based development of HDAC6 inhibitors, screening in N2a cells and in a neuronal model for CMT2F, and preliminary ADMET and pharmacokinetic profiles, resulted in the selection of compound **23d** that possesses improved biochemical, functional, and druglike properties compared to tubastatin A.

KEYWORDS: Selective histone deacetylase 6 inhibitor, Charcot−Marie−Tooth disease, hydroxamic acid, tubulin acetylation, mitochondrial axonal transport, mutant HSPB1-expressing DRG neurons
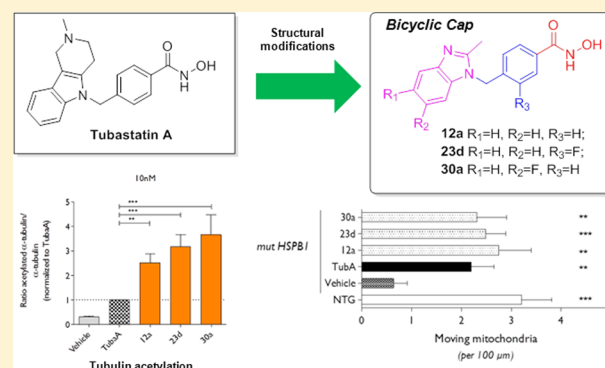
Charcot-Marie-Tooth disease (CMT) is the most commonly inherited disease of the peripheral nervous system, affecting approximately 1 in 2500 individuals in the United States.[1,2] Recently, we have published on the development of transgenic mice that replicate the motor and sensory deficits as seen in CMT2 patients.[3] These mice exhibit defects in mitochondrial trafficking and acetylation of α-tubulin which ultimately contribute to aberrant electrophysiological activity together with altered motor and sensory behavior. Pharmacologic treatment with selective histone deacetylase 6 (HDAC6) inhibitors rescued the disease phenotype and further refined the role of HDAC6 function in this disease.

Covalent post-translational modifications (PTMs) of epigenomic proteins contribute to their biological roles, and thus serve as carriers of epigenetic information from one cell generation to the next.[4] Histone PTMs play key roles in the regulation of transcription, DNA replication, and repair of DNA damage.[5] The major events surrounding epigenetic control are focused on three modes of action: writers, readers, and erasers. The writers are

responsible for adding a variety of PTM marks to histones which include, inter alia, acetylation which is catalyzed by histone acetyltransferases (HATs). Readers refer to the proteins that recognize and bind to these PTM marks thereby mediating their effects, and erasers referred to as histone deacetylases (HDACs) are the enzymes that catalyze the removal of these marks. In the case of acetylated histone lysine residues, HDACs are responsible for catalyzing the hydrolysis of the acetyl mark to provide the unsubstituted lysine residue. The HDAC family consists of at present 18 enzymes which are classified into four subgroups according to their homology to the yeast family. HDAC1, 2, 3, and 8, categorized as class I HDACs according to their homology with yeast Rpd3, are characterized by ubiquitous expression and localization to the nucleus. Class II HDACs show tissue-specific expression and shuttle between the nucleus and cytoplasm.
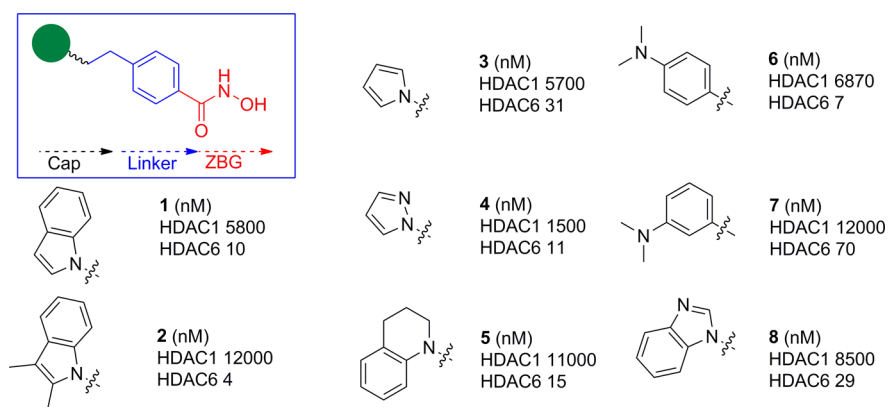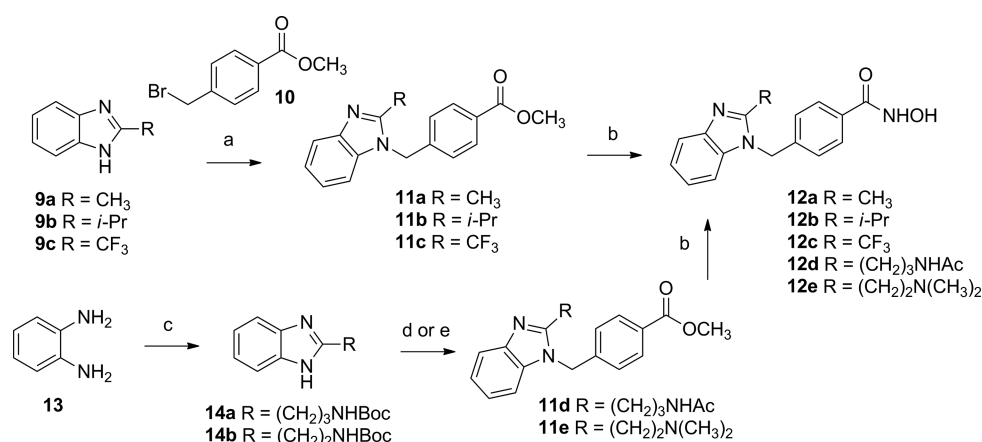
Figure 1. Initial small library of compounds screened to identify possible candidates for HDAC6i lead development.

**Scheme 1. Synthesis of Benzimidazole-Based Analogues**[a]

[a]Reagents and conditions: (a) K_2CO_3, DMF, 80 °C; (b) NaOH, 50 wt % aq. NH_2OH, THF/MeOH (1:1), 0 °C to rt; (c) (i) EDCI, Et_3N, DCM, *N*-Boc-GABA-OH or *N*-Boc-*β*Ala-OH, 0 °C to rt; (ii) AcOH, MeOH, 65 °C; (d) (i) **10**, K_2CO_3, DMF, 80 °C; (ii) HCl, acetone, 50 °C; (iii) Ac_2O, pyridine, DMAP, DCM, 0 °C to rt, for the synthesis of **11d**; (e) (i) **10**, K_2CO_3, DMF, 80 °C; (ii) HCl, acetone, rt; (iii) aq. CH_2O, $NaCNBH_3$, MeOH, rt, for the synthesis of **11e**.

Homologous to yeast Hda1, these enzymes are subdivided in class IIa (HDAC4, 5, 7, and 9) and class IIb (HDAC6 and 10). HDAC11, the only member of the class IV subfamily, shows similarities to the catalytic domains of both class I and II enzymes. Class I, II, and IV HDACs require Zn^{2+} as a cofactor of the deacetylating activity and are also referred to as the conventional HDACs. The sirtuins 1−7 are dependent on nicotinamide adenine dinucleotide for their activity and form class III of the HDACs.

Pharmacologic manipulation of the enzymes involved in regulating protein PTMs, especially those tied to very specific PTM marks, has become an important quest for a number of research groups.[6−8] The discovery of selective small molecule modulators of these enzymes would provide chemical tools to better understand the role of these PTMs at the cellular level, but may also lead to important disease modifiers. Within the HDAC field, there exists a plethora of compounds that are able to block the deacetylase enzymes, and several have made their way to the marketplace for cancer therapy.[9−12] The majority of these HDAC inhibitors (HDACis), however, are not very isoform selective. Many of them inhibit across more than one class of HDAC enzymes and are thus labeled pan-selective. Of the various HDAC isoforms that appear to be promising therapeutic targets for treating humans diseases such as cancer and certain CNS disorders,[13,14] HDAC6 has emerged as a particularly

attractive target, especially in view of the fact that HDAC6 knockout animals remain viable.[15] HDAC6 has no apparent role in the PTM of histone proteins, but rather is involved in regulating the acetylation status of *α*-tubulin, HSP-90, HSF-1, and other protein targets. It is thus better referred to as a lysine deacetylase or KDAC. The development of HDAC6 selective compounds has recently been reviewed.[16] In general, HDACis are composed of three main motifs: a zinc binding group (ZBG), a cap group, and a linker that bridges the previous two (Figure 1). A properly optimized cap group can improve both potency and selectivity, presumably through its ability to engage in appropriate contacts with residues on the enzyme surface.

In our own research on the creation of HDAC6 selective inhibitors, we have reported that use of a phenylhydroxamic acid moiety is particularly effective in achieving isoform selectivity. Certain inhibitors bearing this motif have been shown to possess efficacy as neuroprotective agents,[17] as immunosuppressives,[18] and also as anticancer agents.[19] In this article we report on the structure−activity relationship (SAR) of aryl- and heteroarylhydroxamic acid based inhibitors bearing two different heteroaromatic caps as potent and selective HDAC6 inhibitors with improved efficacy in overcoming mitochondrial deficits seen in an in vitro model for mutant HSPB1-induced CMT2.

Scheme 2. Synthesis of Tetrahydroquinoline-Based Analogues[a]
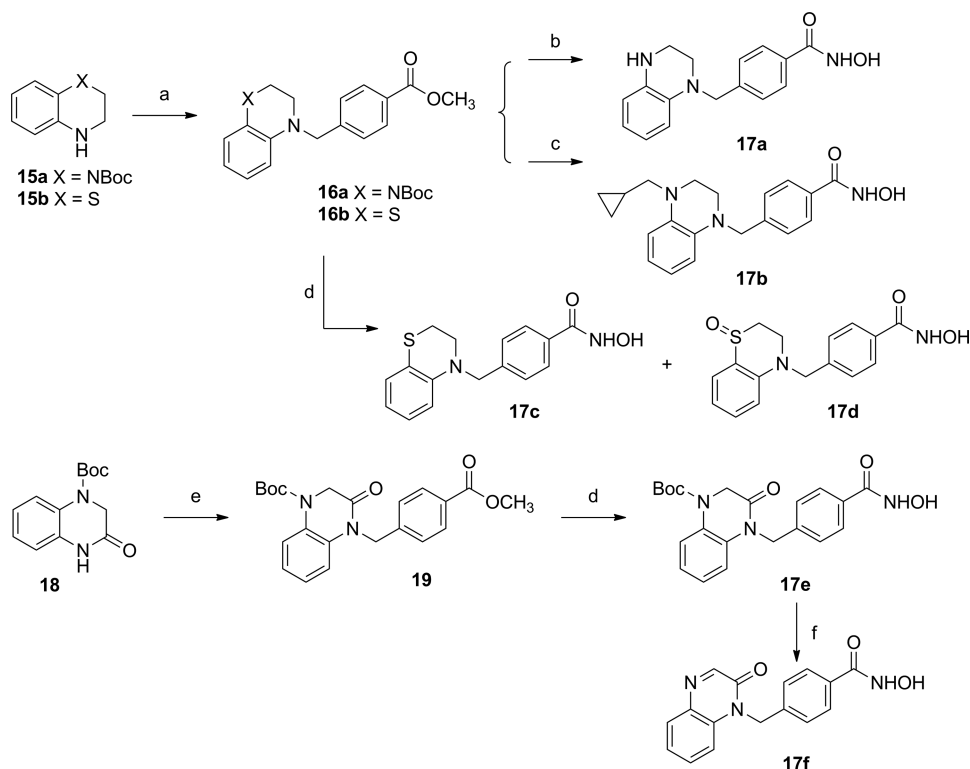
[a]Reagents and conditions: (a) **10**, K$_2$CO$_3$, DMF, 80 °C; (b) (i) NaOH, 50 wt % aq. NH$_2$OH, THF/MeOH (1:1), 0 °C to rt; (ii) TFA/DCM, rt; (c) (i) TFA/DCM, rt; (ii) (bromomethyl)cyclopropane, K$_2$CO$_3$, DMF, 80 °C; (iii) NaOH, 50 wt % aq. NH$_2$OH, THF/MeOH (1:1), 0 °C to rt; (d) (i) NaOH, 50 wt % aq. NH$_2$OH, THF/MeOH (1:1), 0 °C to rt; (ii) TFA/DCM, rt; (e) **10**, NaH, DMF, rt; (f) TFA/DCM, rt.

■ RESULTS AND DISCUSSION

Chemistry. While a solved crystal structure for HDAC6 that might help in understanding the cap group's binding interactions is as yet unavailable, previous work has revealed that a tricyclic cap group[17,18] or a strategically branched urea[19] connected to the phenylhydroxamic acid ZBG was effective in generating reasonably selective HDAC6is. Based on this prior work, we synthesized a small library of HDAC inhibitors (Figure 1) and profiled them for their isoform selectivity by comparing their inhibitory activity at HDAC1 and HDAC6. This initial screen included compounds with both monocyclic and bicyclic caps which are displayed in Figure 1 along with their HDAC1 and HDAC6 IC$_{50}$ values.[17−19] Notably, the tetrahydroquinoline **5** and the benzimidazole **8** emerged as promising starting points for continued SAR studies, as they embrace chemistry scaffolds that are readily amenable to medicinal chemistry efforts.

For the synthesis of benzimidazole analogues, the commercially available benzimidazoles **9a−c** underwent rapid and efficient alkylation with the building block **10** to provide esters **11a−c**, which upon treatment with aqueous NH$_2$OH in basic medium afforded the desired hydroxamic acids **12a−c** efficiently (Scheme 1). To synthesize the analogues **12d** and **12e**, *o*-phenylenediamine (**13**) was coupled with either *N*-Boc-*γ*-aminobutyric acid or *N*-Boc-homoglycine followed by acid-catalyzed cyclization to afford the 2-substituted benzimidazoles **14a** and **14b**, which were then alkylated with **10**. Next, the Boc protecting group was removed with HCl in acetone and the free amine subjected either to reductive amination with aqueous formaldehyde and NaCNBH$_3$ or to acetylation with acetic anhydride to provide the ester intermediates **11d** and **11e**,

respectively. The syntheses were completed as above to afford the desired hydroxamic acids **12d** and **12e**.

Tetrahydroquinoline-based analogues were synthesized by alkylation of the amino group of *N*-Boc-tetrahydroquinoxaline (**15a**) and dihydrobenzothiazine (**15b**) with **10** to afford the esters **16a** and **16b** (Scheme 2). Reaction with aqueous hydroxylamine in the usual manner served to transform the methyl ester to the hydroxamic acid, and in the case of the quinoxaline deprotection with TFA then provided **17a**. To synthesize the *N*-substituted dihydroquinoxaline **17b**, the Boc protecting group of **16a** was first removed with TFA, and the free amine was then alkylated with (bromomethyl)cyclopropane followed by conversion of ester to hydroxamic acid. Synthesis of the dihydrobenzothiazine **17c** in a similar fashion was found to produce a minor amount of the sulfoxide side product **17d**. Ester **19** was obtained by alkylation of the *N*-Boc protected building block **18** with **10** using sodium hydride in DMF. Conversion to the hydroxamic acid **17e** and Boc deprotection with concomitant air oxidation to form **17f** completed the synthesis.

Some SAR centered about the aromatic ring bearing the hydroxamic acid function was also explored, and the synthesis of related analogues is outlined in Scheme 3. Heterocycles **21a,b** were prepared according to a published protocol[20] and were used to alkylate **9a** employing K$_2$CO$_3$ in DMF. Benzyl bromides **21c,d** on reaction with **9a** similarly afforded the esters **22c,d**. Esters **22a−d** were converted to the hydroxamic acids **23a−d** using the standard procedure. The tetrafluorinated benzyl bromide **25** was obtained by NBS bromination of compound **24** and was alkylated with **9a** to afford the ester **22f** and thence the hydroxamic acid **23f**. To synthesize the difluoro analogue **23g**, the THP ether **26** was lithiated with *n*-BuLi followed by

Scheme 3. Synthesis of 2-Methylbenzimidazole Analogues Containing a Modified Linker Region[a]
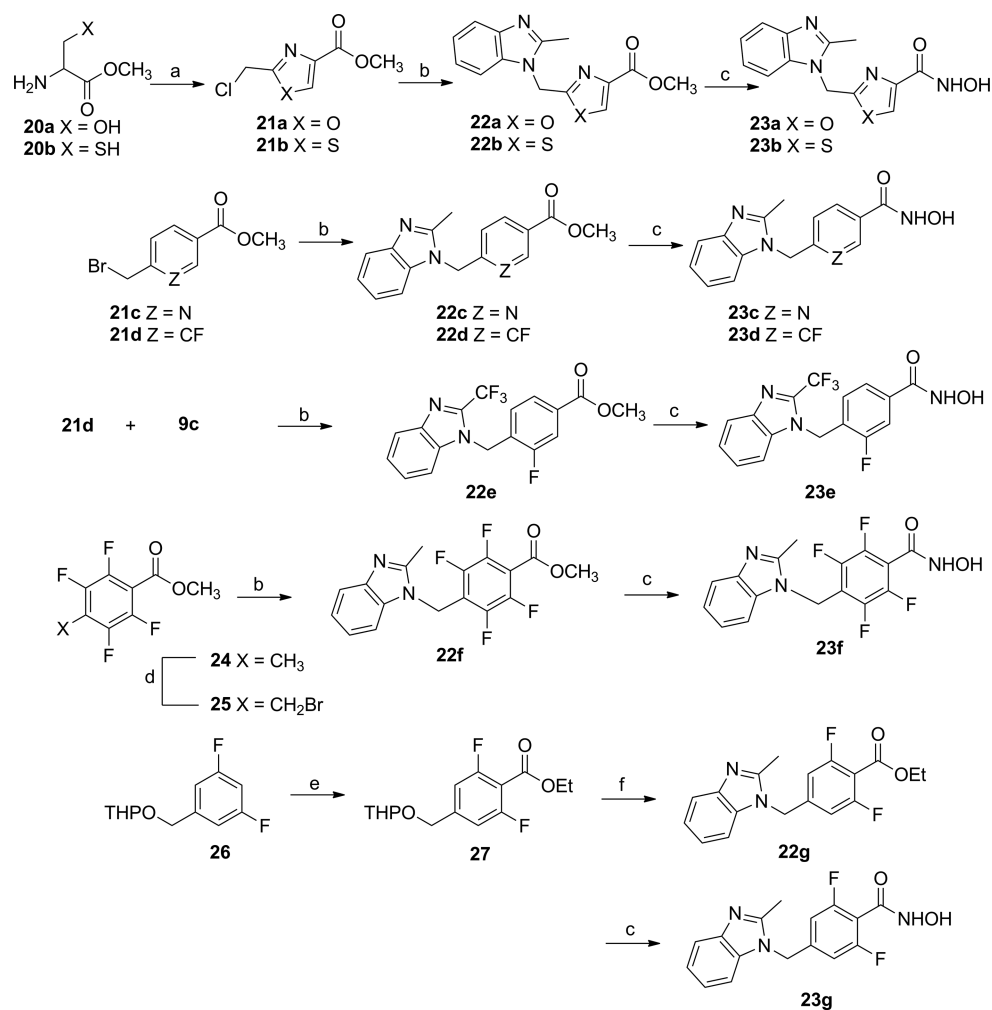
[a]Reagents and conditions: (a) (i) dichloroacetonitrile, NaOMe, MeOH, −10 °C to rt; (ii) NaOMe, MeOH, 0 °C; (b) **9c** (for the synthesis of **22e**) or **9a** (for the synthesis of **22f**), K_2CO_3, DMF, 80 °C; (c) NaOH, 50 wt % aq. NH_2OH, THF/MeOH (1:1), 0 °C to rt; (d) NBS, AIBN, CCl_4, 80 °C; (e) (i) n-BuLi, THF, −78 °C; (ii) EtOCOCl, THF, −78 °C to rt; (f) (i) p-TsOH, MeOH, rt; (ii) MsCl, Et_3N, DCM, rt; (iii) **9a**, K_2CO_3, DMF, 80 °C.

Scheme 4. Synthesis of Fluoro-Substituted Benzimidazole Analogues[a]
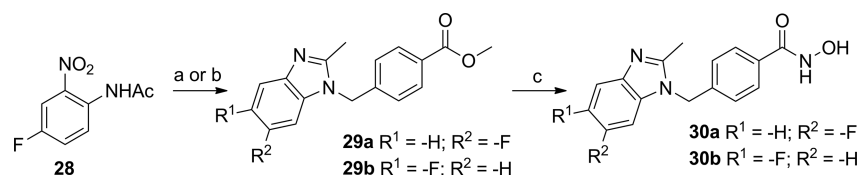
[a]Reagents and conditions: (a) (i) H_2, Pd/C, MeOH, rt; (ii) methyl 4-formylbenzoate, $NaBH(OAc)_3$, AcOH, MeOH, rt; (iii) p-TsOH, toluene, 110 °C, for the synthesis of **29a**; (b) (i) **10**, K_2CO_3, DMF, 80 °C; (ii) Fe, AcOH, EtOH, 80 °C, for the synthesis of **29b**; (c) NaOH, 50 wt % aq. NH_2OH, THF/MeOH (1:1), 0 °C to rt.

quenching with ethyl chloroformate to afford **27**. THP deprotection and in situ activation of the free alcohol as its mesylate allowed for reaction with **9a**. Lastly, the ester was converted to the corresponding hydroxamic acid in the usual manner.

The last series of compounds prepared for the current study examined the effect of appending a fluorine atom to the benzimidazole cap in compound **9a**. Starting with the anilide **28**, a convenient method for accessing both the 5- and 6-fluorinated benzimidazole isomers was developed (Scheme 4). Hydro-

genation of the nitro group of **28** over Pd/C allowed for reductive amination with methyl 4-formylbenzoate. The resulting intermediate was further subjected to ring closure catalyzed by p-TsOH in toluene to afford the 6-fluorinated intermediate **29a**. Alternatively, by first alkylating the amide function of **28** with **10**, and then hydrogenating the nitro group followed by acid-catalyzed cyclization, the 5-fluorinated intermediate **29b** was obtained. The final products **30a** and **30b** were then obtained in the usual manner.

Table 1. Initial HDAC Screening of Bicyclic-Cap Containing Inhibitors[a]
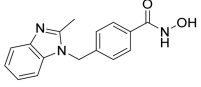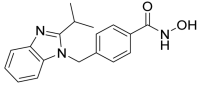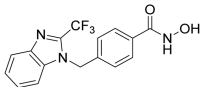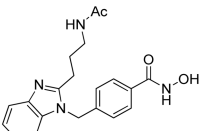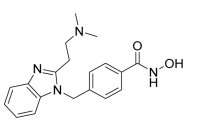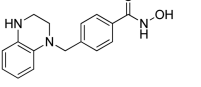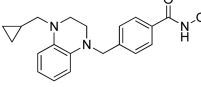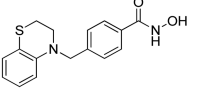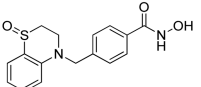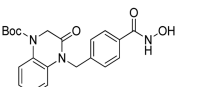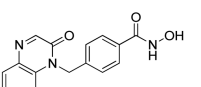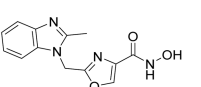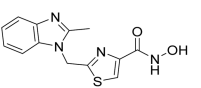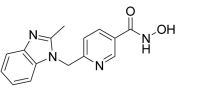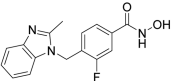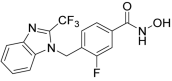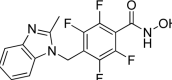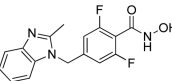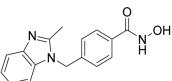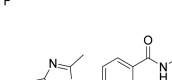
Compound	Structure	IC$_{50}$ (nM)		Selectivity
		HDAC1	HDAC6	HDAC1/HDAC6
12a		8790±1710	9.2±0.5	955
12b		27700±4100	47.0±10.5	589
12c		6340±230	10±0.7	634
12d		14650±350	47.0±15.5	312
12e		52350±10750	125.8±47.2	416
17a		8750±1070	2.9±0.4	3017
17b		6690±270	39.3±0.3	170
17c		7935±25	6.1±0.1	1300
17d		2600±30	2.0±0.1	1300
17e		21950±1550	33.6±1.9	653
17f		1045±5	1.2±0.3	870
23a		NA[b]	3710±500	
23b		NA[b]	8305±905	
23c		27950±2750	77.2±3.7	362

Table 1. continued

Compound	Structure	IC$_{50}$ (nM)		Selectivity
		HDAC1	HDAC6	HDAC1/HDAC6
23d		4320±75	3.0±0.3	1440
23e		24600±100	16.4±0.1	1500
23f		NA^b	3500±270	
23g		NA^b	946±14	
30a		2920±10	5.2±0.4	562
30b		5875±165	6.4±0.1	918
TSA^c		16.8±1.5	1.5±0.2	11

^{a}IC$_{50}$ values are the mean of two experiments ± standard deviation obtained from curve-fitting of a 10-point enzymatic assay starting from 30 μM with 3-fold serial dilution (Reaction Biology Corp, Malvern, PA). ^{b}No inhibitory activity. ^{c}Trichostatin A.

HDAC Isoform Inhibition. To measure the in vitro activity of the bicyclic-capped HDAC6is, assays for HDAC inhibition were performed against HDAC6 and one member of the class 1 isoforms, HDAC1, to establish a preliminary selectivity profile. IC$_{50}$'s for these two isoforms along with their selectivity index are summarized in Table 1.

Modifications to the 2-position of the benzimidazole cap had significant effects on HDAC inhibition. Increasing the substituent size from hydrogen (**8**) to methyl (**12a**) resulted in a 3-fold increase in HDAC6 inhibitory potency (from 29 to 9 nM) with nearly 1000-fold selectivity versus HDAC1. The bulkier isopropyl derivative **12b** exhibited reduced potency at HDAC6. Analogue **12c** bearing a CF$_3$ group, which has approximately the size of an ethyl group, showed activity comparable to that of **12a**. Effects of a hydrogen bond donor/ acceptor group were examined with compounds **12d** and **12e**. The acetamidopropyl derivative **12d** was equipotent to **12b**, suggesting the steric effects control compound potency with little influence from the polar substituent. The N,N-dimethylaminoethyl group at the 2-position of the benzimidazole cap in **12e** caused a further reduction in potency, suggesting that a positively charged amino group at this site is deleterious. Thus, a small, lipophilic group or hydrogen atom appears to be favored at this site.

The next series of compounds were based on the tetrahydroquinoline **5**. Incorporation of an additional nitrogen atom into the molecule to afford the quinoxaline **17a** led to an improvement in potency with an IC$_{50}$ of 3 nM. Alkylation of the free nitrogen atom of the quinoxaline ring with a cyclopropylmethyl group was not favorable, as the potency of **17b**

at HDAC6 fell to 39 nM. The dihydrobenzothiazine **17c** proved to be a potent HDAC6 inhibitor with an IC$_{50}$ of 6 nM, and the sulfoxide **17d** obtained as a side product in the synthesis of **17c** displayed an even better potency (IC$_{50}$ = 2 nM). N-Boc protected **17e** was less potent than the deprotected compound **17f** (IC$_{50}$ of 34 vs 1 nM, respectively). Comparing analogue pairs **17a/b** and **17e/f**, the free nitrogen atom positioned atop the cap group was clearly preferred, suggesting a possible favorable interaction of the amino and imine groups with the surface of the enzyme leading to improved enzyme inhibition. Steric interactions from the bulky Boc and cyclopropylmethyl groups may also play a role in this observed activity.

The development of tubastatin A has demonstrated the importance of incorporating an aromatic ring into the linker for establishing potency and selectivity for HDAC6 compared to compounds with purely aliphatic linkers.[17] However, further modifications to this motif have remained largely unexplored. Using the 2-methylbenzimidazole cap from **12a** as the common element, a small library of compounds with modified aryl and heteroaryl groups in their linkers was examined (**23a−g**). Incorporation of oxazole (compound **23a**) and thiazole (compound **23b**) rings in the linkers resulted in HDAC6is with activities merely in the micromolar range, a >400- and >900- fold reduction compared to **12a**, respectively. These results suggest that a 6-membered aromatic ring is favored. Incorporation of a pyridine ring into the linker as in **23c** also resulted in a drop in HDAC6 inhibition (IC$_{50}$ = 77 nM), however, not to the same extent as seen with the 5-membered ring heterocycles. The dipole moment of the pyridine ring and/or its protonation state may be responsible for its poorer engagement with the active site

of the enzyme. It is likely that the difference in the orientation of the ZBG when mounted on a five- or six-membered ring also has an impact on activity. Addition of a fluorine atom to the 3-position of the aryl linker as in **23d** provided a 3-fold increase in potency (HDAC6, IC_{50} = 3 nM) in comparison to **12a**, and this analogue was found to be >1400-fold selective over HDAC1. The electron withdrawing effect of the fluorine atom in **23d** should enhance the acidity of the hydroxamate, which would favor deprotonation of the oxygen atom with formation of a negatively charged group for interaction with zinc. Combining the linker present in **21b** with the cap present in **9c** led to **23e** with fluorine substituents in both the cap and linker. Analogue **23e** had an HDAC6 inhibitory potency (IC_{50} = 16 nM) that is similar to that of **12c**, thus indicating that the size of the substituent on the cap plays the more prominent role in determining activity. By comparison, the hydroxamic acid ZBG of **23d** has a calculated pK_a of 8.4 (calculated by Precepta ADME software, ACD Laboratories), and the increased lipophilicity resulting from fluorination may improve binding energies correlating with improved HDAC6 inhibition. The difluoro compound **23g** has two fluorine atoms located ortho to the hydroxamate group and has a much reduced potency of 960 nM at HDAC6. This reduced activity may stem from steric interactions which are discussed in further detail in the modeling section that follows. It was also not surprising that the tetrafluoro-substituted analogue **23f** showed even weaker HDAC6 inhibitory potency than **23g**. While the added fluorine atoms make the hydroxamic acid even more acidic (a calculated pK_a of 6.5), thus favoring deprotonation of the oxygen atom and its interaction with zinc, the steric interactions of the fluorine atoms again alter the geometry of the phenylhydroxamate.

Substitution of H by F on the cap, either at the 6-position (compound **30a**) or the 5-position (compound **30b**) generated potent HDAC6 inhibitors (IC_{50}'s of 5 and 6 nM, respectively) with high selectivity relative to HDAC1 (Table 1). While these substitutions would presumably not impact the pK_a of the hydroxamic acid compared to the linker substitutions, slight gains in lipophilicity may be beneficial for improving active-site engagement. Additionally, multipolar interactions involving the fluorine on the inhibitor with the surface of the enzyme cannot be ruled out.

Three analogues (**12a**, **23d**, and **30a**) were selected for full HDAC profiling at all of the 11 class I, II, and IV HDACs, and these results are summarized in Table 2. In general, these compounds displayed excellent selectivity versus the class I and IV members with the lone exception of HDAC8 (class I), which is unique in that the literature suggests that this particular isoform has a high degree of plasticity and can accommodate diverse HDACi structures.[21−25] These three analogues all displayed lower selectivity against the class IIa isoforms (HDAC4, 5, 7, and 9). However, as the contribution of the deacetylase activity of these isoforms to cellular events is currently under debate, the measured activity may not be of any consequence in terms of in vitro or in vivo activity.[26] Lastly, the difference in potency for all three compounds between HDAC6 and HDAC10 is notable, as HDAC10 is the other member comprising the class IIb subcategory with HDAC6.

Modeling Studies. Despite the lack of a solved X-ray structure, the use of molecular modeling has aided in developing an SAR for HDAC6is.[17] This model has been useful in identifying the utility of the aromatic linker portion and provides further insights into defining characteristics of potent and selective compounds. The inhibitors generated were subjected to

Table 2. Complete Characterization of Three Selected HDACis at all 11 class I, II, and IV HDAC Enzymes[a]

HDAC isozyme (IC_{50}, nM)	12a	23d	30a	TubaA HCl
HDAC1	4240	8960	4360	4440
HDAC2	11 000	20 300	7430	11 800
HDAC3	10 900	12 500	10 000	7150
HDAC4	1010	470	1460	1640
HDAC5	406	182	397	582
HDAC6	4.65	0.81	3.12	3.17
HDAC7	87.2	32.2	211	234
HDAC8	305	176	368	499
HDAC9	345	70.1	463	527
HDAC10	12 000	20 400	11 800	11 900
HDAC11	9810	12 900	7490	12 500

[a]Compounds were tested in singlet 10-dose IC_{50} mode with 3-fold serial dilution starting at a concentration of 1 μM against HDAC6 and 100 μM against the other 10 HDAC isoforms (Reaction Biology Corp, Malvern, PA).

molecular modeling studies to better rationalize their diverse potency.

In regard to the interactions with the zinc ion, docking results revealed a consistent binding mode for the most active compounds in which the hydroxamic acid assumes the expected bidentate chelation with the zinc cofactor. In active compounds, the hydroxamic moiety and aromatic linker portion lie in the same plane, thus adopting a pose by which the linker benzene ring contributes to $\pi-\pi$ stacking with Phe680 in addition to engaging in apolar contacts with surrounding hydrophobic residues, namely Pro501, Val650, and Leu749 (see Figure 2 for **23d** and Figure S1A for **17f**). The key role of such a planar arrangement can explain the lower potency of the derivatives in which the hydoxamate-bearing phenyl ring also contains two ortho-fluorine atoms (i.e., **23f** and **23g**). Indeed, the steric hindrance exerted by these substituents forces the hydroxamate to be roughly perpendicular to the phenyl ring, thus preventing an optimal arrangement for bivalent chelation with the zinc atom in addition to causing steric clashes with other surrounding residues in the catalytic site (as seen in Figure S1B for **23g**). As suggested above and further supported by Figure S1C for **23a**, the incorporation of a 5-membered aromatic ring in the linker markedly impacts the location of the hydroxamic acid which is unable to conveniently approach the zinc ion. In contrast, the incorporation of a pyridine ring (as present in **23c**, complex not shown) does not influence the optimal pose of the hydroxamic acid, thus confirming that the lower potency of this compound may be ascribable to the destabilizing effect of the pyridine ring nitrogen that prefers to be located away from the benzene ring π-cloud.[27]

Figure 2A depicts compound **23d** docked within the active site of HDAC6, with the benzimidazole situated on the cavity rim where it can stabilize $\pi-\pi$ stacking with Phe680. Additionally, in this orientation, the N^3 nitrogen can elicit a weak H-bond with Ser568. The methyl group fits into a small subpocket that aids in cap alignment. In concert with the biochemical data, the C^2-position in compounds **12a−e** likely plays an important role in the observed potency at HDAC6. Along these lines, the desmethyl analogue **7** shows reduced inhibitory potency, further suggesting that this position aids in proper orientation of the bicyclic cap group at the protein surface.

Figure 2B illustrates another potential interaction leading to the increased potency observed against HDAC6. The fluorine
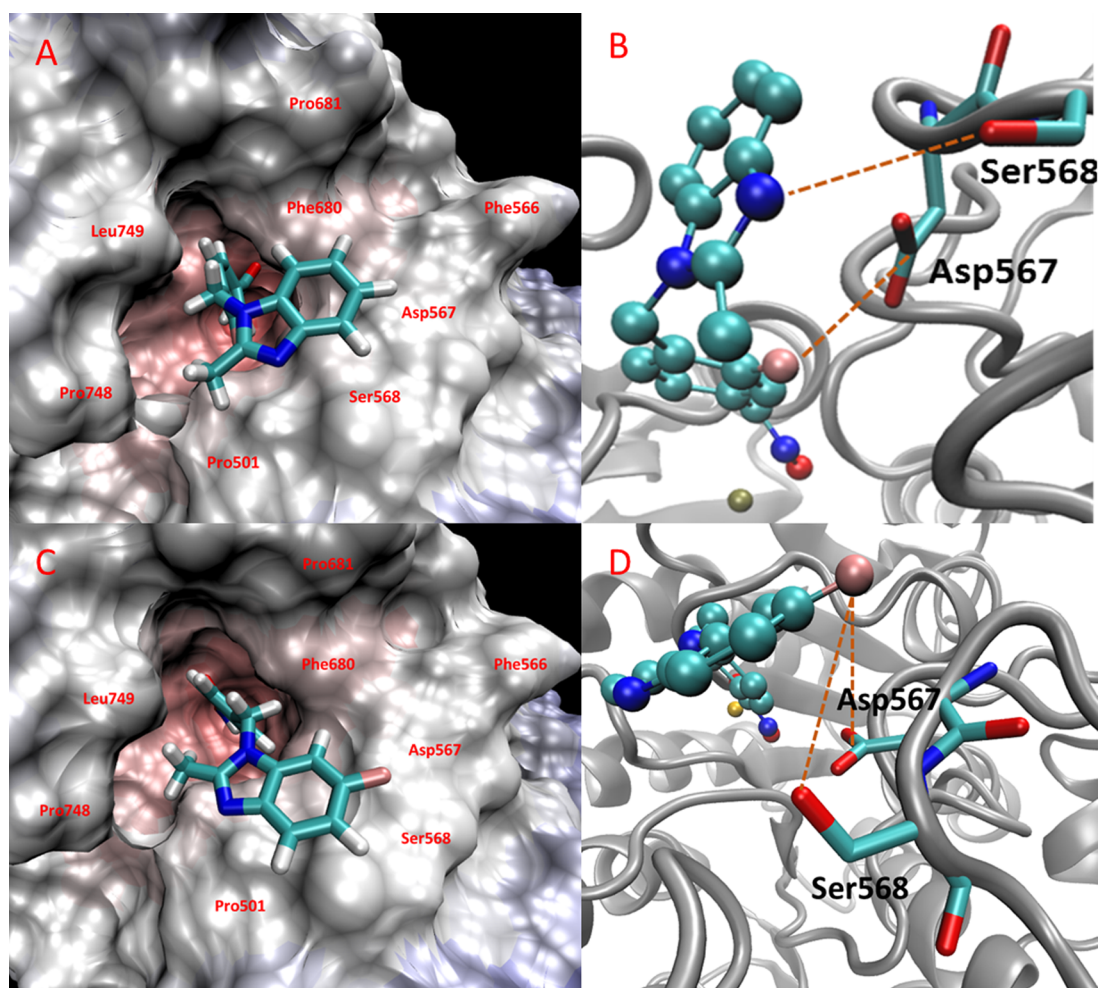
Figure 2. Putative complexes for **23d** (A and B) and **30a** (C and D) in the HDAC6 active site.

Table 3. Summary of Evaluation of Potency and Selectivity of Candidate HDAC6 Inhibitors in N2a Cells[a]

	ratio acetylated α-tubulin/α-tubulin (1 μM)				Ratio acetylated α-tubulin/α-tubulin (10 nM)				ratio acetylated H3/H4 (1 μM)		
	N	mean	SEM	Dunnett	N	mean	SEM	mean	N	mean	SEM	Dunnett
vehicle	20	0.03	0.01	***	20	0.31	0.04	ns	4	1.00	0.00	
TubaA	3	1.00	0.00		4	1.00	0.00		10	1.87	0.22	ns
12a	3	1.03	0.13	ns	3	2.63	0.51	**	3	0.95	0.17	ns
12b	3	0.61	0.07	ns	3	0.32	0.10	ns	3	2.01	0.39	ns
12c	3	1.35	0.46	ns	3	1.55	0.45	ns	3	0.62	0.10	ns
12d	4	0.24	0.06	**	4	0.39	0.15	ns	4	0.88	0.15	ns
17a	4	0.36	0.16	*	4	0.40	0.13	ns	4	1.82	0.64	ns
17b	4	0.36	0.10	*	4	0.43	0.15	ns	4	1.78	0.82	ns
17c	4	1.04	0.19	ns	4	0.75	0.16	ns	4	1.52	0.42	ns
17d	4	1.11	0.14	ns	4	0.93	0.24	ns	4	1.45	0.39	ns
17e	3	0.77	0.02	ns	3	0.53	0.11	ns	3	2.82	0.53	***
17f	4	0.82	0.19	ns	4	1.36	0.43	ns	4	2.68	1.00	ns
23c	4	0.28	0.06	*	4	0.61	0.30	ns	4	1.51	0.41	ns
23d	3	1.20	0.28	ns	3	2.80	0.48	***	3	0.77	0.17	ns
23e	3	1.24	0.07	ns	3	1.00	0.47	ns	3	0.92	0.18	ns
23f	4	0.03	0.00	***	4	0.32	0.10	ns	4	1.87	0.58	ns
23g	4	0.23	0.09	**	4	0.35	0.11	ns	4	1.09	0.20	ns
30a	3	1.66	0.34	*	3	3.87	1.08	***	3	1.14	0.13	ns
30b	3	1.02	0.10	ns	3	1.84	0.31	ns	3	2.02	0.40	ns

[a]All compounds were tested at 1 μM and 10 nM and the acetylation of α-tubulin and histone 3 was quantified by WB. Dunnett's multiple comparison test. *$p < 0.05$, **$p < 0.001$, ***0.0001.

Figure 3. Compounds **12a**, **23d**, and **30a** selectively inhibit HDAC6 in N2a cells. (A and B) Incubation of N2a cells with 1 μM or 10 nM of the HDAC6 inhibitors results in an increased acetylation of α-tubulin. (C and D) WBs were quantified by measuring the ratio of acetylated α-tubulin to the total amount of α-tubulin. The values were normalized to tubastatin A (TubaA) within each experiment. Graphs represent means with SEM. Dunnett's multiple comparison test. *$p < 0.05$, **$p < 0.001$, ***$p < 0.0001$. N = 4.

atom present in compound **23d** approaches the side-chain carboxylate of Asp567, where it can stabilize both a halogen bond, when it approaches a carboxyl oxygen atom, and/or an orthogonal multipolar interaction when it approaches the carboxyl carbon depending on the presumably flexible mutual orientation between fluoro atom and carboxylate group. The average distance between the fluorine of **23d** and the car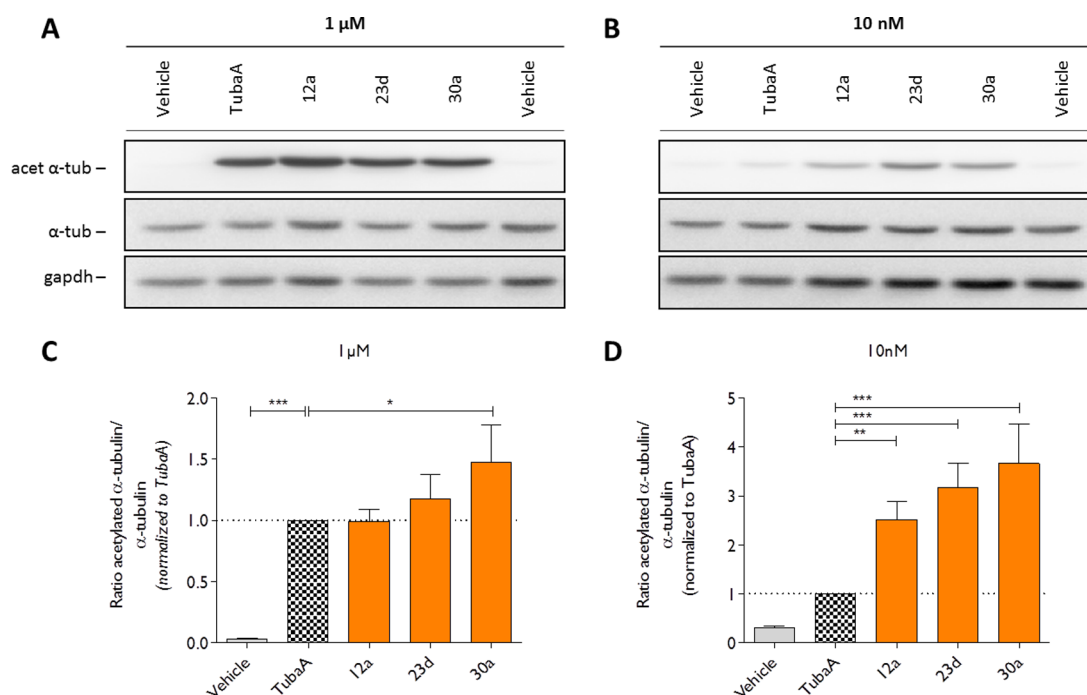bon atom of the carboxyl group (3.70 Å) is in accord with published data regarding multipolar interactions involving fluorine atoms.[28]

The beneficial role of the fluorine atom in stabilizing the computed complexes is further supported by the putative complex formed with **30a**, which arranges its cap so as to direct the fluorine atom between Asp567 and Ser568 (as seen in Figure 2C and D). In this case, the fluorine atom can elicit halogen bonding with Ser568 plus engage in multipolar interactions with Asp567. Moreover, **30a** is seen to conserve all of the previously mentioned hydrophobic interactions at the rim of the cavity, which may be further strengthened by the lipophilic fluorine atom. Additionally, docking results suggest that the possible interaction between the −NH− group of some of the quinoxaline derivatives and Ser568 can explain their excellent potency. The quinoxaline **17f** appears to be further stabilized by a $\pi-\pi$ stacking interaction between the ligand's lactam group and Asp567. This type of carboxyl-peptide plane stacking interaction has been found to occur between buried aspartate residues and to play a role in stabilizing protein folding as recently discussed by Yao et al.[29]

Screening. In search of a potential pharmacological therapy for CMT2, a screening paradigm was set up consisting of 2 phases for a more detailed characterization of the compounds as selective inhibitors for the deacetylating function of HDAC6. To study the compounds in a more complex cellular environment Neuro-2a (N2a) cells were used to measure the potency and selectivity of the HDAC6 inhibitors. It was shown previously that tubastatin A is effective in restoring deficits found in a mutant HSPB1-induced mouse model for CMT2. Therefore, during the next step of the screening process the candidate inhibitors would be tested for their ability to restore defects seen in mutant HSPB1 DRG neuron cultures.

Screening for Selective and Improved HDAC6 Inhibitors in N2a Cells. To identify compounds that inhibit the deacetylating function of HDAC6, the ability to increase the acetylated α-tubulin/total α-tubulin ratio in N2a cells was tested. The results are summarized in Table 3. In terms of compound selectivity for HDAC6 in comparison to other HDAC enzymes, this was quantified by assessing the changes in the acetylated histone 3(H3)/histone 4(H4) ratio on Western Blot (WB) analysis. Using tubastatin A as a reference, only inhibitors with equal or improved properties were selected for further screening. In addition we chose to work with one high (1 μM) and one suboptimal concentration (10 nM) as a second criterion. In this more complex cellular environment, **12d**, **17a**, **17b**, **23c**, **23f**, and **23g** were not able to increase the acetylation of α-tubulin even at the high concentration tested, and therefore these compounds were not advanced to the next phases of the screening (Table 3 and Figure S2). On the contrary, **30a** significantly increased the levels of acetylated α-tubulin compared to tubastatin A. In a second step of our analysis, using a suboptimal concentration (10 nM) only 3 compounds showed increased potency compared to tubastatin A (Table 3 and Figure S3). In addition, **12a**, **23d**, and **30a** did not alter the acetylation of histone 3 (Table 3 and Figure S4). In combination with their high potency toward HDAC6, these compounds are thus interesting candidates to move forward for further characterization (Table 3 and Figure 3).

12a, 23d, and 30a Improve Mitochondrial Axonal Transport in Mutant HSPB1 DRG Neurons. The second phase of the screening focused on the potential of these compounds to serve as a pharmacological therapy for CMT2. Testing was
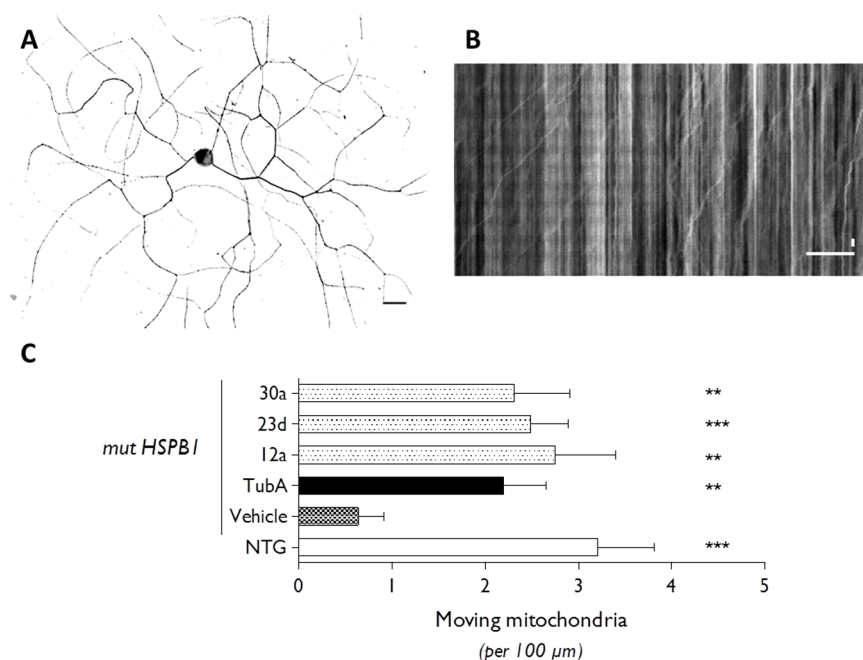
Figure 4. Axonal transport deficits are rescued by several selective HDAC6 inhibitors. (A) DRG neuron cultured from an adult transgenic HSPB1 mouse is stained for neuronal marker β3-tubulin. Scale bar 50 μm. (B) Axonal transport is measured by tracking the mitochondrial movement within one neurite from each DRG neuron resulting in a kymograph. Vertical lines indicate stationary mitochondria while lines deflecting to the right or left represent anterograde or retrograde moving particles. Horizontal scale bar 20 μm. Vertical scale bar 10 s. (C) Comparing mitochondrial axonal transport in DRG neurons cultured from nontransgenic (NTG) or transgenic (mut HSPB1) mice shows significantly decreased movement in DRG neurons expressing mutant HSPB1. After treatment of the transgenic DRG neurons with 100 nM of the candidate HDAC6 inhibitors, the number of moving mitochondria per 100 μm of neurite was quantified. Similar to the positive control tubastatin A, **12a**, **23d**, and **30a** are able to restore the movement of mitochondria. Graph represents mean values with SEM. Dunn's multiple comparison test. **$p < 0.01$, ***$p < 0.0001$. $N = 18-27$ for 3–5 mice.

conducted in cultured DRG neurons from a CMT2 mouse model. These mice exhibit the neuron-specific overexpression of S135F mutant HSPB1 and develop motor and sensory deficits from the age of 6 months on. The cultured DRG neurons from symptomatic mice show abnormal axonal transport of mitochondria and decreased levels of acetylated α-tubulin. Tubulin acetylation is an important component in the axonal transport of several cargoes since it ensures the binding of the motor proteins to the microtubule network.[30] Treatment of the mutant DRG neuron cultures with an inhibitor specifically affecting the deacetylating function of HDAC6 rescues the axonal defects.[3] Therefore, the aim of this screening phase focused on the functionality of the selected compounds, that is, their ability to restore the defects in mutant HSPB1 DRG neuron cultures by inhibiting HDAC6.

The DRG neurons were thus treated overnight with 100 nM of **12a**, **23d**, **30a**, or tubastatin A (Figure 4). The mitochondrial movement was measured by labeling the organelles with a mitochondrial dye prior to obtaining a time lapse video during 200 s. Analysis of the kymographs shows decreased movement of mitochondria in vehicle treated cells as compared to DRG neurons cultured from NTG mice. This mitochondrial transport can be improved by selectively inhibiting the deacetylating function of HDAC6 by applying tubastatin A, **12a**, **23d**, or **30a**. The data obtained thus indicate that these three compounds are not only selective and potent HDAC6 inhibitors, but that they are also able to restore deficits seen in an in vitro model for CMT2. In particular, all three compounds were observed to promote mitochondrial transport better than tubastatin A.

In vitro ADMET Assays and Pharmacokinetic Profiles. Based upon the HDAC6 selectivity data of the top three compounds, together with their tubulin acetylation activity, their ability to promote mitochondrial transport, as well as concerns about the poor solubility of **12a** (70 μM in PBS at pH 7.4), we chose to carry out in vitro ADMET studies and in vivo PK profiling on compound **23d** in order to gain a better understanding of its suitability for future studies in the CMT animals. The results are summarized in Table 3. In comparison to tubastatin A, **23d** showed similar aqueous solubility and slightly improved Caco-2 cell permeability (A−B) with a reduced efflux ratio. Notably, compound **23d** demonstrated a considerable improvement in metabolic stability using human hepatocytes although its half-life in mouse hepatocytes was similar to that of tubastatin A. The plasma stability data were quite similar for **23d** and tubastatin A in both human and mouse. In terms of interactions with a panel of cytochrome P450s **23d** showed only weak inhibition of 3A4-T with an IC$_{50}$ value of 36 μM, while no inhibition of the other CYPs was observed.

The intravenous and oral plasma pharmacokinetic parameters of **23d** in male CD1 mice are also summarized in Table 4. These data again revealed some improvements for **23d** compared with tubastatin A, including a considerable improvement in the C$_{max}$ when administered orally and a reduced clearance rate. The bioavailability of **23d** expressed as the F% is also superior to that found for tubastatin A and is about 21 compared to about 6 for tubastatin A.

■ CONCLUSIONS

A focused chemical library was assembled to probe the pharmacophore of HDAC6 inhibitors based on the general chemical scaffold shown in Figure 1. By utilizing a bicyclic cap as the structural scaffold, we identified several analogues that showed comparable or improved potency compared to

Table 4. In Vitro ADMET and Plasma PK Parameters for 23d[a]

compd		tubastatin A	**23d**
aqueous solubility (PBS, pH 7.4, μM)		301	302
Caco-2 permeability (pH 7.4 × 10^{-6} cm/s)	A–B	2.00	3.89
	B–A	19.7	13.2
liver microsomes stability, $T_{1/2}$ (min)	human	1520	1944
	mouse	303	285
hepatocyte stability, $T_{1/2}$ (min)	human	88	1488
	mouse	30	40
plasma stability remaining percentage (%, 120 min)	human	96.4	93.4
	mouse	83.0	87.9
CYP Inhibition, IC_{50} (μM)	1A2	>50	>50
	2C9	>50	>50
	2C19	>50	>50
	2D6	16	>50
	3A4-M	>50	>50
	3A4-T	>50	36
mouse PK (iv dose 3 mg/kg; po dose 30 mg/kg)[b]			
iv	Cl (mL/min/kg)	222	34
	V_{dss} (L/kg)	4.14	0.382
	$t_{1/2}$ (h)	0.351	0.851
	$AUC_{(0-\infty)}$ (h·ng/mL)	227	1483
po[c]	t_{max} (h)	0.25	0.25
	C_{max} (ng/mL)	135 ± 36	4367 ± 470
	$AUC_{(0-\infty)}$ (h*ng/mL)	134 ± 12	3105 ± 84
	F (%)	5.88 ± 0.53	20.9 ± 0.53

[a]These ADMET and PK parameters were profiled by Pharmaron, Inc., Irvine, CA. [b]Compounds were tested in a formulation composed of 5% DMSO in "10% HP-β-CD in saline" (adjusted pH with 0.5 M HCl). [c]Data are presented as the mean ± SD from three male CD1 mice.

tubastatin A for HDAC6 while maintaining excellent selectivity compared to HDAC1. Further screening was set up not only to characterize the potency and selectivity of this library but also to identify HDAC6 inhibitors that exhibit improved pharmacokinetics in comparison to tubastatin A. Specifically, derivatives **12a**, **23d**, and **30a**, all bearing a bicyclic cap, demonstrated improved efficiency in inducing tubulin acetylation compared to tubastatin A. In an *in vitro* model for mutant HSPB1-induced CMT2 **12a**, **23d**, and **30a** restored mitochondrial axonal transport defects characteristic of this disease. The PK data in conjunction with the preliminary ADMET results suggest that it would be reasonable to advance compound **23d** into mouse studies using the HSPB1 mutant animals as well as other CMT mutants that are available.

◼ METHODS

General Information. ^{1}H and ^{13}C NMR spectra were obtained on a 400/100 MHz Bruker spectrometer, except where noted otherwise, using the solvent residual peak as the internal reference (chemical shifts: $CDCl_3$, δ 7.26/77.0; CD_3OD, 3.31/49.15; DMSO-d_6, 2.50/39.52). The following abbreviations for multiplicities were used: s = singlet, d = doublet, t = triplet, q = quartet, m = multiplet, and br = broad. TLC plates (Merck silica gel 60 F_{254}, 250 μm thickness) were used to monitor reaction progress, and spots were visualized under a UV lamp. Low-resolution mass spectrometry (LRMS) was carried out on an Agilent 1946A LC-MSD and high-resolution mass spectrometry (HRMS) on a Shimadzu IT-TOF instrument. In either case, the mobile phase

consisted of an acetonitrile−water mixture (containing 0.1% formic acid). Flash chromatography was performed on a CombiFlash Rf system (Teledyne ISCO) with silica gel cartridges. Preparative HPLC was used in the purification of all final compounds using a Shimadzu preparative LC under the following conditions: column, ACE 5AQ (150 × 21.2 mm), 5 μm particle size; mobile phase, 8−100% MeOH/water containing 0.05% TFA at a flow rate of 17 mL/min for 30 min; UV detection at 254 and 280 nm. Where indicated, StratoSpheres PL-HCO$_3$ MP resin (Agilent Technologies) was used to neutralize the TFA salts obtained during preparative HPLC purification. Analytical HPLC was carried out on an Agilent 1100 series instrument under the following conditions: column, Luna 5 C18(2), pore size 100 Å, dimensions 150 × 4.6 mm, particle size 5 μm; mobile phase, 10−100% MeOH/water containing 0.05% TFA at a flow rate of 1.4 mL/min for 18 min; UV detection at 254 nM. The purity of all tested compounds was >95%, as determined by analytical HPLC.

4-(1-Indolylmethyl)-N-hydroxybenzamide (1). To NaH (60% by weight in mineral oil, 171 mg, 4.27 mmol) suspended in anhydrous DMF (20 mL) under argon was added at 0 °C indole (500 mg, 4.27 mmol) dissolved in anhydrous DMF (12 mL). The reaction was stirred for 15 min at 0 °C, then methyl 4-(bromomethyl)benzoate (978 mg, 4.27 mmol) was added as a solution in anhydrous DMF (8 mL). The reaction was stirred for 2 h at 70 °C and then quenched by the addition of H_2O (30 mL). The organic products were extracted with EtOAc (3 × 30 mL), and the combined organic layers were washed with H_2O (2 × 30 mL) and brine (15 mL), dried over sodium sulfate, filtered, and concentrated under vacuum. The crude product was purified by flash chromatography (0−50% EtOAc/hexanes) to yield methyl 4-(1-indolylmethyl)benzoate as a white solid (860 mg, 76%). ^{1}H NMR (400 MHz, $CDCl_3$): δ 8.05 (A part of an AA′XX′ multiplet, $J_{AX} + J_{AX'}$ = 8.2 Hz, 2H), 7.79 (d, J = 6.9 Hz, 1H), 7.33−7.16 (m, 6H), 6.70 (d, J = 3.1 Hz, 1H), 5.35 (s, 2H), 3.97 (s, 3H). ^{13}C NMR (100 MHz, $CDCl_3$): δ 166.4, 142.6, 136.0, 129.8 (2C), 129.3, 128.6, 128.1, 126.4 (2C), 121.7, 120.9, 119.6, 109.4, 101.9, 51.9, 49.5. ESI HRMS calcd. for $C_{17}H_{16}NO_2$: $[M + H]^+$, m/z 266.1176. Found: 266.1182.

Methyl 4-(1-indolylmethyl)benzoate (840 mg, 3.17 mmol) was dissolved in MeOH (10 mL) and added to a mixture of $NH_2OH \cdot HCl$ (1.32 g, 19.0 mmol) and MeOH (10 mL). Subsequently, a 25% by weight solution of NaOMe in MeOH (5.48 g, 25.4 mmol) was added. The mixture was stirred for 2 h at 0 °C, allowed to warm to room temperature, and stirred for an additional 22 h. When the reaction was complete as evidenced by TLC, it was quenched by the addition of a 10% solution of TFA in DCM (15 mL). Solids were filtered off, and the filter cake was washed with MeOH (10 mL). The combined filtrate and washing were concentrated under vacuum, and the residue was dissolved in DMF and purified by preparative HPLC to yield the title compound as a white solid after lyophilization (443 mg, 53%). ^{1}H NMR (400 MHz, DMSO-d_6): δ 11.14 (s, 1H), 9.0 (br, 1H), 7.67, 7.23 (AA′XX′ multiplet, $J_{AX} + J_{AX'}$ = 8.1 Hz, 4H), 7.56 (d, J = 7.8 Hz, 1H), 7.52 (d, J = 3.1 Hz, 1H), 7.42 (d, J = 8.1 Hz, 1H), 7.09 (t, J = 7.4 Hz, 1H), 7.02 (t, J = 7.3 Hz, 1H), 6.50 (d, J = 3.0 Hz, 1H), 5.48 (s, 2H). ^{13}C NMR (100 MHz, DMSO-d_6): δ 163.9, 141.4, 135.7, 129.2 (2C), 128.3, 127.1 (2C), 126.8 (2C), 121.2, 120.5, 119.2, 110.1, 101.1, 48.7. ESI HRMS calcd for $C_{16}H_{15}N_2O_2$: $[M + H]^+$, m/z 267.1128. Found: 267.1137.

4-[(2,3-Dimethyl-1-indolyl)methyl]-N-hydroxybenzamide (2). Methyl 4-[(2,3-dimethyl-1-indolyl)methyl]benzoate was prepared from 2,3-dimethylindole (500 mg, 3.44 mmol) following a procedure similar to that described for the preparation of the intermediate ester used in the synthesis of **1** and isolated as a viscous yellow oil (652 mg, 65%). ^{1}H NMR (400 MHz, $CDCl_3$): δ 7.93, 7.02 (AA′XX′ multiplet, $J_{AX} + J_{AX'}$ = 8.2 Hz, 4H), 7.55 (m, 1H), 7.18−7.08 (m, 3H), 7.02 (d, J = 8.2 Hz, 2H), 5.34 (s, 2H), 3.89 (s, 3H), 2.30 (s, 3H), 2.27 (s, 3H). ^{13}C NMR (100 MHz, $CDCl_3$): δ 166.8, 143.5, 136.3, 132.2, 130.1 (2C), 129.2, 128.7, 126.0 (2C), 121.0, 119.1, 118.1, 108.6, 107.4, 52.1, 46.4, 10.1, 8.9. ESI HRMS calcd. for $C_{19}H_{20}NO_2$: $[M + H]^+$, m/z 294.1489. Found: 294.1503.

The title compound was synthesized from methyl 4-[(2,3-dimethyl-1-indolyl)methyl]benzoate (632 mg, 2.15 mmol) using a procedure similar to that described for the preparation of **1** and isolated as a white solid (487 mg, 77%). ^{1}H NMR (400 MHz, DMSO-d_6): δ 11.13 (br s,

1H), 9.0 (br s, 1H), 7.66 (A part of an AA′XX′ multiplet, $J_{AX} + J_{AX'}$ = 8.2 Hz, 2H), 7.45 (d, J = 6.9 Hz, 1H), 7.32 (d, J = 7.3 Hz, 1H), 7.05−6.97 (m, 4H), 5.43 (s, 2H), 2.27 (s, 3H), 2.22 (s, 3H). ^{13}C NMR (100 MHz, DMSO-d_6): δ 164.0, 141.9, 136.0, 132.5, 131.6, 128.2, 127.2 (2C), 126.0 (2C), 120.5, 118.6, 117.7, 109.1, 106.0, 45.5, 9.8, 8.6. ESI HRMS calcd. for $C_{18}H_{19}N_2O_2$: $[M + H]^+$, m/z 295.1441. Found: 295.1453.

4-(1-Pyrrolylmethyl)-N-hydroxybenzamide (3). Methyl 4-(1-pyrrolylmethyl)benzoate was prepared from pyrrole (150 mg, 2.24 mmol) following a procedure similar to that described for the preparation of the intermediate ester used in the synthesis of **1** (substituting KO^{t}Bu for NaH) and isolated as a clear viscous oil (432 mg, 90%). ^{1}H NMR (400 MHz, CDCl$_3$): δ 8.01, 7.17 (AA′XX′ multiplet, $J_{AX} + J_{AX'}$ = 8.3 Hz, 2H), 6.72−6.71 (m, 2H), 6.25−6.24 (m, 2H), 5.13 (s, 2H), 3.91 (s, 3H). ^{13}C NMR (100 MHz, CDCl$_3$): δ 166.7, 143.4, 130.0 (2C), 129.5, 126.7 (2C), 121.2 (2C), 108.9 (2C), 53.0, 52.1. ESI LRMS: $[M + H]^+$, m/z 216.1.

The title compound was synthesized from methyl 4-(1-pyrrolylmethyl)benzoate (400 mg, 1.86 mmol) using a procedure similar to that described for the preparation of **1** and isolated as a white solid (225 mg, 56%). ^{1}H NMR (400 MHz, CD$_3$OD): δ 7.69, 7.19 (AA′XX′ multiplet, $J_{AX} + J_{AX'}$ = 8.3 Hz, 4H), 6.74−6.72 (m, 2H), 6.12−6.11 (m, 2H), 5.16 (s, 2H). ^{13}C NMR (100 MHz, CD$_3$OD): δ 168.0, 144.6, 132.8, 128.5 (2C), 128.2 (2C), 122.3 (2C), 109.6 (2C), 53.6. ESI HRMS calc. for $C_{12}H_{13}N_2O_2$: $[M + H]^+$, m/z 217.0977. Found: 217.0974.

4-(1-Pyrazolylmethyl)-N-hydroxybenzamide (4). Methyl 4-(1-pyrazolylmethyl)benzoate was prepared from pyrazole (150 mg, 2.20 mmol) following a procedure similar to that described for the preparation of the intermediate ester used in the synthesis of **1** (substituting KO^{t}Bu for NaH) and isolated as a viscous yellow oil (387 mg, 81%). ^{1}H NMR (400 MHz, CDCl$_3$): δ 7.98, 7.20 (AA′XX′ multiplet, $J_{AX} + J_{AX'}$ = 8.2 Hz, 4H), 7.55 (s, 1H), 7.40 (d, J = 2.0 Hz, 1H), 6.29 (d, J = 1.9 Hz, 1H), 5.35 (s, 2H), 3.87 (s, 3H). ^{13}C NMR (100 MHz, CDCl$_3$): δ 166.5, 141.7, 139.8, 129.9 (2C), 129.6, 129.4, 127.2 (2C), 106.1, 55.3, 52.0. ESI HRMS calcd. for $C_{12}H_{13}N_2O_2$: $[M + H]^+$, m/z 217.0972. Found: 217.0969.

The title compound was synthesized from methyl 4-(1-pyrazolylmethyl)benzoate (387 mg, 1.79 mmol) using a procedure similar to that described for the preparation of **1**. After purification by preparative HPLC, residual TFA was neutralized using PL-HCO$_3$ MP resin and the neutral product isolated as a white solid after lyophilization (251 mg, 65%). ^{1}H NMR (400 MHz, CD$_3$OD): δ 7.74−7.73 (m, 1H), 7.72, 7.27 (AA′XX′ multiplet, $J_{AX} + J_{AX'}$ = 8.4 Hz, 4H), 7.55 (d, J = 1.5 Hz, 1H), 6.37−6.36 (m, 1H), 5.43 (s, 2H). ^{13}C NMR (100 MHz, CD$_3$OD): δ 167.9, 142.5, 140.9, 133.2, 132.0, 128.7 (2C), 128.6 (2C), 107.3, 55.9. ESI HRMS calcd. for $C_{11}H_{12}N_3O_2$: $[M + H]^+$, m/z 218.0924. Found: 218.0917.

4-[(1,2,3,4-Tetrahydro-1-quinolyl)methyl]-N-hydroxybenzamide (5). A solution of 1,2,3,4-tetrahydroquinoline (126 μL, 1.00 mmol) and 4-formylbenzoic acid methyl ester (164 mg, 1.00 mmol) in toluene (5 mL) was stirred under reflux overnight. The solution was cooled to room temperature and concentrated under vacuum. The crude imine intermediate was taken up in THF (5 mL) containing AcOH (69 μL, 1.20 mmol). The solution was stirred at room temperature for 30 min, followed by the addition of NaBH(OAc)$_3$ (318 mg, 1.50 mmol). The mixture was stirred at room temperature overnight. Water was added, and the product was extracted into EtOAc (3 × 15 mL). The combined organic layers were washed with brine, dried over sodium sulfate, filtered, and concentrated under vacuum. The crude product was purified by flash chromatography (0−30% EtOAc/hexanes) to yield 4-(1,2,3,4-dihydro-1-quinolylmethyl)benzoic acid methyl ester as a light yellow oil (156 mg, 56%). ^{1}H NMR (400 MHz, CDCl$_3$): δ 7.98, 7.33 (AA′XX′ multiplet, $J_{AX} + J_{AX'}$ = 8.5 Hz, 4H), 7.00−6.93 (m, 2H), 6.59 (t, J = 7.3 Hz, 1H), 6.41 (d, J = 8.2 Hz, 1H), 4.51 (s, 2H), 3.90 (s, 3H), 3.37 (t, J = 5.6 Hz, 2H), 2.83 (t, J = 6.3 Hz, 2H), 2.06−1.99 (m, 2H). ^{13}C NMR (100 MHz, CDCl$_3$): δ 167.0, 145.3, 144.7, 130.0 (2C), 129.1, 128.8, 127.2, 126.5 (2C), 122.4, 116.2, 111.0, 55.3, 52.0, 50.1, 28.1, 22.4. ESI LRMS: $[M + H]^+$, m/z 282.1.

Solid NaOH (89 mg, 2.22 mmol) was dissolved in a 50% aqueous solution of NH$_2$OH (1 mL) at 0 °C. A solution of methyl 4-[(1,2,3,4-

tetrahydroquinolin-1-yl)methyl]benzoic acid methyl ester (156 mg, 0.54 mmol) in 1:1 THF/MeOH (6 mL) was added dropwise to the vigorously stirred solution. Upon complete addition, the ice bath was removed, and the reaction was allowed to stir for 15 min. The mixture was then acidified to pH 5 with 2 N HCl and concentrated under vacuum. The was dissolved in DMF and purified by preparative HPLC to yield the desired compound as a white solid after lyophilization (90 mg, 58%). ^{1}H NMR (400 MHz, DMSO-d_6): δ 11.14 (br s, 1H), 8.99 (br s, 1H), 7.70, 7.30 (AA′XX′ multiplet, $J_{AX} + J_{AX'}$ = 8.0 Hz, 4H), 6.89 (d, J = 7.3 Hz, 1H), 6.85 (t, J = 8.0 Hz, 1H), 6.46 (t, J = 7.3 Hz, 1H), (d, J = 8.2 Hz, 1H), 4.51 (s, 2H), 3.38−3.33 (m, 2H), 2.75−2.72 (m, 2H), 1.94−1.91 (m, 2H). ^{13}C NMR (100 MHz, DMSO-d_6): δ 164.2, 144.9, 142.5, 131.3, 128.8, 127.1 (2C), 126.9, 126.5 (2C), 121.7, 115.4, 110.6, 54.0, 49.6, 27.6, 21.8. ESI HRMS calcd. for $C_{17}H_{19}N_2O_2$: $[M + H]^+$, m/z 283.1441. Found: 283.1435.

4-[4-(Dimethylamino)benzyl]-N-hydroxybenzamide (6). 4-(Dimethylamino)phenylboronic acid (165 mg, 1.00 mmol), methyl 4-(bromomethyl)benzoate (275 mg, 1.20 mmol), tetrakis-(triphenylphosphine)palladium(0) (23 mg, 0.02 mmol), and K$_2$CO$_3$ (290 mg, 2.10 mmol) were placed in a dry, sealed tube under an argon atmosphere. Diglyme (4 mL) and H$_2$O (2 mL) were added through a rubber septum which was immediately replaced by the tube's screw-on cap. The mixture was heated to 100 °C and stirred for 4 h. Then, the mixture was diluted with H$_2$O (20 mL), and the organic products were extracted with DCM (3 × 15 mL). The combined organic layers were washed with brine (15 mL), dried over sodium sulfate, filtered, and concentrated under vacuum. The residue was purified by flash chromatography (0−10% MeOH/DCM) to yield methyl 4-[4-(dimethylamino)benzyl]benzoate as an orange oil (211 mg, 78%). ^{1}H NMR (400 MHz, CD$_3$OD): δ 7.96, 7.36 (AA′XX′ multiplet, $J_{AX} + J_{AX'}$ = 8.4 Hz, 4H), 7.62, 7.48 (AA′XX′ multiplet, $J_{AX} + J_{AX'}$ = 8.7 Hz, 4H), 4.13 (s, 2H), 3.90 (s, 3H), 3.31 (s, 6H). ^{13}C NMR (100 MHz, CD$_3$OD): δ 168.5, 147.5, 144.4, 142.8, 132.2 (2C), 131.0 (2C), 130.2 (2C), 129.7, 121.8 (2C), 52.7, 47.1 (2C), 42.0. ESI LRMS: $[M + H]^+$, m/z 271.1.

The title compound was synthesized from methyl 4-[4-(dimethylamino)benzyl]benzoate (211 mg, 0.78 mmol) using a procedure similar to that described for the preparation of **1** and isolated as a white solid (140 mg, 66%). ^{1}H NMR (400 MHz, CD$_3$OD): δ 7.69, 7.31 (AA′XX′ multiplet, $J_{AX} + J_{AX'}$ = 8.2 Hz, 4H), 7.53, 7.42 (AA′XX′ multiplet, $J_{AX} + J_{AX'}$ = 8.6 Hz, 4H), 4.09 (s, 2H), 3.25 (s, 6H). ^{13}C NMR (100 MHz, CD$_3$OD): δ 168.1, 146.1, 143.8, 143.2, 132.1 (2C), 131.7, 130.3 (2C), 128.6 (2C), 121.4 (2C), 46.9 (2C), 41.9. ESI HRMS calcd. for $C_{16}H_{19}N_2O_2$: $[M + H]^+$, m/z 271.1441. Found: 271.1448.

4-[3-(Dimethylamino)benzyl]-N-hydroxybenzamide (7). Methyl 4-[3-(dimethylamino)benzyl]benzoate was prepared from 3-(dimethylamino)phenylboronic acid (165 mg, 1.00 mmol) following a procedure similar to that described for the preparation of the intermediate ester used in the synthesis of **6** and isolated as a clear oil (254 mg, 94%). ^{1}H NMR (400 MHz, CDCl$_3$): δ 7.97, 7.24 (AA′XX′ multiplet, $J_{AX} + J_{AX'}$ = 8.1 Hz, 4H), 7.41−7.39 (m, 1H), 7.35−7.27 (m, 2H), 7.18 (d, J = 7.5 Hz, 1H), 4.06 (s, 2H), 3.89 (s, 3H), 3.13 (s, 6H). ^{13}C NMR (100 MHz, CDCl$_3$): δ 166.9, 144.9, 144.5, 143.1, 130.6, 130.0 (2C), 128.9 (2C), 128.8, 128.6, 119.9, 117.5, 52.1, 45.6 (2C), 41.6. ESI LRMS: $[M + H]^+$, m/z 271.1.

The title compound was synthesized from methyl 4-[3-(dimethylamino)benzyl]benzoate (254 mg, 0.94 mmol) using a procedure similar to that described for the preparation of **1** and isolated as a white solid (117 mg, 46%). ^{1}H NMR (400 MHz, CD$_3$OD): δ 7.70 (A part of an AA′XX′ multiplet, $J_{AX} + J_{AX'}$ = 8.2 Hz, 2H), 7.53−7.46 (m, 3H), 7.38−7.32 (m, 3H including 7.34, B part of an AA′XX′ multiplet, $J_{AX} + J_{AX'}$ = 8.3 Hz, 2H), 4.12 (s, 2H), 3.27 (s, 6H). ^{13}C NMR (100 MHz, CD$_3$OD): δ 168.1, 145.8, 145.3, 145.1, 131.9, 131.7, 131.2, 130.3 (2C), 128.7 (2C), 121.7, 119.0, 46.9 (2C), 42.3. ESI HRMS calcd. for $C_{16}H_{19}N_2O_2$: $[M + H]^+$, m/z 271.1441. Found: 271.1450.

4-(1-Benzimidazolylmethyl)-N-hydroxybenzamide TFA Salt (8). To a round-bottom flask charged with methyl 4-(bromomethyl)-benzoate (458 mg, 2.00 mmol) in DMF (8 mL) were added benzimidazole (236 mg, 2.00 mmol) and K$_2$CO$_3$ (276 mg, 2.00 mmol) in succession. The resulting mixture was allowed to stir at 80 °C for 16 h, and the reaction was monitored by TLC. Upon completion, the

reaction was quenched with H$_2$O (20 mL), and the mixture was extracted with EtOAc (3 × 20 mL). The combined organic extracts were washed with H$_2$O (2 × 15 mL) and brine (15 mL), dried over sodium sulfate, filtered, and concentrated under vacuum. The crude product was purified by flash chromatography (0−10% MeOH/DCM) to yield methyl 4-(1-benzimidazolylmethyl)benzoate as an off-white waxy solid (501 mg, 94%). ^{1}H NMR (400 MHz, CDCl$_3$): δ 8.00 (A part of an AA′XX′ multiplet, $J_{AX} + J_{AX'}$ = 8.2 Hz, 2H), 7.96 (s, 1H), 7.84 (d, J = 7.8 Hz, 1H), 7.32−7.19 (m, 5H including 7.22, B part of an AA′XX′ multiplet, $J_{AX} + J_{AX'}$ = 8.2 Hz, 2H), 5.41 (s, 2H), 3.90 (s, 3H). ^{13}C NMR (100 MHz, CDCl$_3$): δ 166.4, 144.0, 143.2, 140.5, 133.8, 130.3 (2C), 130.2, 126.9 (2C), 123.3, 122.5, 120.6, 109.9, 52.2, 48.4. ESI LRMS: [M + H]$^+$, m/z 267.1.

Solid NaOH (112 mg, 2.79 mmol) was dissolved in a 50% aqueous solution of NH$_2$OH (1 mL) at 0 °C. A solution of methyl 4-(1-benzimidazolylmethyl)benzoate (93 mg, 0.35 mmol) in 1:1 THF/MeOH (6 mL) was added dropwise with vigorous stirring. Upon complete addition, the ice bath was removed, and the reaction was allowed to stir for 15 min. The reaction was then quenched with AcOH (0.20 mL, 3.49 mmol), and the mixture was concentrated under vacuum. The residue was dissolved in DMF and purified by preparative HPLC to yield the desired compound as a white solid after lyophilization (81 mg, 87%). ^{1}H NMR (400 MHz, DMSO-d_6): δ 11.2 (br s, 1H), 9.36 (s, 1H), 7.84−7.82 (m, 1H), 7.78−7.72 (m, 3H including 7.75, A part of an AA′XX′ multiplet, $J_{AX} + J_{AX'}$ = 8.0 Hz, 2H), 7.52−7.43 (m, 4H including 7.49, B part of an AA′XX′ multiplet, $J_{AX} + J_{AX'}$ = 8.2 Hz, 2H), 5.74 (s, 2H). ^{13}C NMR (100 MHz, DMSO-d_6): δ 163.6, 158.3 (q, J = 335 Hz, TFA anion), 142.8, 138.1, 135.1, 132.7, 131.7, 127.8 (2C), 127.4 (2C), 125.0 (2C), 116.6, 112.5, 48.6. ESI LRMS: [M + H]$^+$, m/z 268. ESI HRMS calcd. for C$_{15}$H$_{14}$N$_3$O$_2$: [M + H]$^+$, m/z 268.1081. Found: 268.1080.

Methyl 4-[(2-Methyl-1-benzimidazolyl)methyl]benzoate (11a). General Procedure A. To a round-bottom flask charged with 2-methylbenzimidazole (9a, 264 mg, 2.0 mmol) and methyl 4-(bromomethyl)benzoate (10, 458 mg, 2.0 mmol) in DMF (10 mL) was added K$_2$CO$_3$ (553 mg, 4.0 mmol). The resulting mixture was allowed to stir for 2 h at 80 °C. The mixture was cooled to room temperature and after addition of water (15 mL) extracted with EtOAc (3 × 15 mL). The combined organic extracts were washed with brine (40 mL), dried over sodium sulfate, and concentrated under vacuum. The crude product was purified by flash chromatography (0−5% MeOH/DCM), and the title compound was obtained as an off-white waxy solid (298 mg, 53%). ^{1}H NMR (400 MHz, CDCl$_3$): δ 7.97, 7.10 (AA′XX′ multiplet, $J_{AX} + J_{AX'}$ = 8.4 Hz, 4H), 7.75 (d, J = 7.8 Hz, 1H), 7.30−7.15 (m, 3H), 5.34 (s, 2H), 3.89 (s, 3H), 2.55 (s, 2H). ^{13}C NMR (100 MHz, CDCl$_3$): δ 166.3, 151.6, 142.6, 140.8, 135.2, 130.2 (2C), 129.8, 126.0 (2C), 122.3, 122.1, 119.1, 109.1, 52.1, 46.7, 13.8. ESI LRMS: [M + H]$^+$, m/z 281.1.

Methyl 4-[(2-Isopropyl-1-benzimidazolyl)methyl]benzoate (11b). Synthesized according to General Procedure A from 2-isopropylbenzimidazole (9b, 209 mg, 1.3 mmol), 10 (299 mg, 1.3 mmol), and K$_2$CO$_3$ (359 mg, 2.6 mmol); off-white waxy solid (239 mg, 64%). ^{1}H NMR (400 MHz, CDCl$_3$): δ 7.97, 7.09 (AA′XX′ multiplet, $J_{AX} + J_{AX'}$ = 8.5 Hz, 4H), 7.81 (d, J = 7.9 Hz, 1H), 7.26 (td, J = 7.5 Hz, 1.5 Hz, 1H), 7.19 (td, J = 7.5 Hz, 1.1 Hz, 1H), 7.15 (d, J = 8 Hz, 1H), 5.42 (s, 2H), 3.89 (s, 3H), 3.12 (septuplet, J = 6.9 Hz, 1H), 1.39 (d, J = 6.8 Hz, 6H). ^{13}C NMR (100 MHz, CDCl$_3$): δ 166.5, 160.0, 142.7, 141.3, 135.1, 130.3 (2C), 129.9, 126.0 (2C), 122.5, 122.2, 119.6, 109.4, 52.2, 46.5, 26.6, 21.7. ESI LRMS: [M + H]$^+$, m/z 309.2.

Methyl 4-[[2-(Trifluoromethyl)-1-benzimidazolyl]methyl]-benzoate (11c). Synthesized according to General Procedure A from 2-(trifluoromethyl)benzimidazole (9c, 200 mg, 1.07 mmol), 10 (245 mg, 1.07 mmol), and K$_2$CO$_3$ (296 mg, 2.14 mmol); light yellow oil (295 mg, 82%). ^{1}H NMR (100 MHz, CDCl$_3$): δ 8.00, 7.16 (AA′XX′ multiplet, $J_{AX} + J_{AX'}$ = 8.0 Hz, 4H), 7.93 (d, J = 8 Hz, 1H), 7.43−7.32 (m, 2H), 7.27 (m, 1H), 5.60 (s, 2H), 3.90 (s, 3H). ^{13}C NMR (100 MHz, CDCl$_3$): δ 166.4, 141.2, 140.8 (d, J = 38 Hz), 139.8, 135.4, 130.3 (2C), 130.2, 126.2 (2C), 125.8, 124.0, 121.9, 119.1 (d, J = 270 Hz), 110.8, 52.2, 48.1. ESI LRMS: [M + H]$^+$, m/z 335.1.

tert-Butyl [3-(2-Benzimidazolyl)propyl]carbamate (14a). To a round-bottom flask charged with 4-[(N-tert-butoxycarbonyl)amino]-butyric acid (500 mg, 2.46 mmol) in dry DCM (10 mL) under an atmosphere of argon was added Et$_3$N (1.0 mL, 7.36 mmol) followed by 1-ethyl-3-[3-(dimethylamino)propyl]carbodiimide (EDCI, 706 mg, 3.69 mmol) at 0 °C. The mixture was allowed to stir for 10 min. Next, *o*-phenylenediamine (13, 266 mg, 2.46 mmol) was added at once, and the resulting solution was allowed to stir at room temperature for 16 h. The reaction was quenched with water (10 mL), and lipophilic materials were extracted into DCM (3 × 10 mL). The combined organic extracts were washed with brine (20 mL), dried over sodium sulfate, and concentrated under vacuum. The residue was dissolved in AcOH (7 mL) and stirred at 65 °C for 1 h. After cooling to room temperature, the mixture was basified with saturated aqueous sodium bicarbonate solution, and the organics were extracted with DCM (2 × 15 mL). The combined organic extracts were washed with brine (20 mL), dried over sodium sulfate, and concentrated under vacuum. The product was obtained as a yellow waxy solid (433 mg, 64%) and was used without further purification. ^{1}H NMR (400 MHz, CD$_3$OD): δ 7.48, 7.18 (AA′XX′ multiplet, $J_{AX} + J_{AX'}$ = 9.2 Hz, 4H), 3.13 (d, J = 6.8 Hz, 2H), 2.90 (d, J = 7.6 Hz, 2H), 1.98 (quintuplet, J = 7.2 Hz, 2H), 1.42 (s, 9H). ^{13}C NMR (100 MHz, CD$_3$OD): δ 158.7, 156.4, 139.7, 123.4 (4C), 115.5, 80.2, 40.9, 29.8, 28.9 (3C), 27.2. ESI LRMS (m/z): [M + H]$^+$ = 276.2.

tert-Butyl [2-(2-Benzimidazolyl)ethyl]carbamate (14b). The title compound was synthesized according to the procedure used for 14a starting from N-(tert-butoxycarbonyl)-β-alanine (1.00 g, 5.78 mmol). All spectral data are in agreement with those published in the literature.[31] ^{1}H NMR (400 MHz, DMSO-d_6): δ 12.21 (s, 1H), 7.52 (d, J = 6.7 Hz, 1H), 7.40 (d, J = 7.7 Hz, 1H), 7.17−7.07 (m, 2H), 6.95−6.94 (m, 1H), 3.40−3.35 (m, 2H), 2.93 (t, J = 7.3 Hz, 2H), 1.37 (s, 9H). ^{13}C NMR (100 MHz, DMSO-d_6): δ 155.5, 152.8, 143.3, 134.2, 121.5, 120.8, 119.1, 110.8, 77.7, 38.6, 29.3, 28.2 (3C). ESI LRMS: [M + H]$^+$, m/z 262.1.

Methyl 4-[[2-(3-Acetamidopropyl)-1-benzimidazolyl]methyl]-benzoate (11d). This compound was synthesized according to General Procedure A from 14a (433 mg, 1.57 mmol), 10 (360 mg, 1.57 mmol), and K$_2$CO$_3$ (434 mg, 3.14 mmol) in DMF (8 mL). The reaction was worked up in the usual manner. The crude alkylation product was dissolved in acetone (7 mL), and 3 equiv of conc. HCl was added. The solution was stirred at 50 °C overnight, then concentrated under vacuum and basified with 10% aqueous sodium bicarbonate solution (20 mL). The organics were extracted with DCM (3 × 10 mL), and the combined organic layers were dried over sodium sulfate and evaporated to obtain crude amine (458 mg, 90%). To an aliquot of this material (135 mg, 0.42 mmol) in DCM (5 mL) were added Et$_3$N (76 μL, 0.51 mmol), Ac$_2$O (51 μL, 0.54 mmol), and DMAP (5 mg, 0.04 mmol) under an atmosphere of argon at 0 °C. The resulting solution was allowed to stir at room temperature for 24 h. The reaction was quenched with 1 N NaOH solution (5 mL), and the organics were extracted with DCM (3 × 10 mL). The combined organic layers were washed with brine (15 mL), dried over sodium sulfate, and concentrated under vacuum. The crude product was purified by flash chromatography (0−10% MeOH/DCM) to afford the desired product as a brown oil (53 mg, 35%). ^{1}H NMR (400 MHz, CDCl$_3$): δ 7.97 (d, J = 8.4 Hz, 2H), 7.75 (d, J = 8.0 Hz, 1H), 7.34−7.14 (m, 3H), 7.08 (d, J = 8.1 Hz, 2H), 6.82 (br s, 1H), 5.38 (s, 2H), 3.89 (s, 3H), 3.33 (dd, J = 12.3, 6.0 Hz, 2H), 2.89 (t, J = 7.0 Hz, 2H), 2.10−2.00 (m, 2H), 1.87 (s, 3H). ^{13}C NMR (100 MHz, CDCl$_3$): δ 170.4, 166.4, 154.6, 142.2, 140.8, 135.2, 130.3 (2C), 129.9 (2C), 126.1, 122.8, 122.4, 119.1, 109.5, 52.2, 46.6, 39.2, 26.5, 25.2, 23.1. ESI LRMS: [M + H]$^+$, m/z 366.1.

Methyl 4-[[2-[2-(Dimethylamino)ethyl]-1-benzimidazolyl]-methyl]benzoate (11e). Synthesized according to General Procedure A from 14b (444 mg, 1.70 mmol), 10 (390 mg, 1.70 mmol), and K$_2$CO$_3$ (470 mg, 3.40 mmol) in DMF (8 mL). The reaction was worked up in the usual manner. The crude alkylation product was dissolved in acetone (7 mL), and 3 equiv of conc. HCl was added. The solution was stirred at 50 °C overnight, then concentrated under vacuum and basified with 10% aqueous sodium bicarbonate solution (20 mL). The organics were extracted with DCM (3 × 10 mL), and the combined organic layers were

dried over sodium sulfate and evaporated to obtain crude amine. To an aliquot of this material (131 mg, 343 μmol) in MeOH (4 mL) were added AcOH (100 μL), NaCNBH$_3$ (43 mg, 686 μmol), and 37% aqueous formaldehyde solution (100 μL) sequentially under an atmosphere of argon at 0 °C. The resulting solution was allowed to stir at room temperature for 4.5 h. The solution was acidified with 1 N HCl (10 mL) and washed with ethyl acetate (2 × 10 mL). The aqueous layer was basified with 2N NaOH and extracted with ethyl acetate (3 × 10 mL). The combined organic layers were washed with brine (15 mL), dried over sodium sulfate, and concentrated under vacuum. The crude product was purified by flash chromatography (0−15% MeOH/DCM) to afford the title compound as a brown oil (88 mg, 76%). ^{1}H NMR (400 MHz, CDCl$_3$): δ 7.97, 7.11 (AA′XX′ multiplet, $J_{AX} + J_{AX'}$ = 8.2 Hz, 4H), 7.76 (d, J = 7.6 Hz, 1H), 7.29−7.15 (m, 3H), 5.42 (s, 2H), 3.89 (s, 3H), 3.01−2.97 (m, 2H), 2.85−2.81 (m, 2H), 2.26 (s, 6H). ^{13}C NMR (100 MHz, CDCl$_3$): δ 166.4, 153.4, 142.6, 141.0, 135.2, 130.3 (2C), 129.9, 126.1 (2C), 122.6, 122.3, 119.4, 109.3, 57.1, 52.2, 46.7, 45.3 (2C), 26.1. ESI LRMS: [M + H]$^+$, m/z 338.2.

N-Hydroxy-4-[2-methyl-1-benzimidazolyl)methyl]benzamide (12a). General Procedure B. In a round-bottom flask, NaOH (157 mg, 3.94 mmol) was dissolved in 50% aqueous NH$_2$OH (1 mL, approximately 50 equiv) at 0 °C. A solution of **11a** (276 mg, 984 μmol) in 1:1 THF/MeOH (6 mL) was added dropwise, and stirring was continued for 30 min while warming to room temperature. The solution was neutralized with 6 N HCl and concentrated under vacuum. The residue was purified by preparative HPLC to afford the title compound as an off-white solid after lyophilization (105 mg, 38%). ^{1}H NMR (400 MHz, DMSO-d_6): δ 11.30 (br s, 1H), 7.84−7.78 (m, 2H), 7.76, 7.41 (AA′XX′ multiplet, $J_{AX} + J_{AX'}$ = 8.3 Hz, 4H), 7.57−7.48 (m, 2H), 5.79 (s, 2H), 2.90 (s, 3H). ^{13}C NMR (100 MHz, DMSO-d_6): δ 163.6, 151.9, 138.0, 133.3, 132.7, 132.5, 127.5 (2C), 127.1 (2C), 124.8, 124.6, 115.2, 112.1, 46.9, 12.3. ESI HRMS calcd. for C$_{16}$H$_{16}$N$_3$O$_2$: [M + H]$^+$, m/z 282.1237. Found: 282.1228.

N-Hydroxy-4-[(2-isopropyl-1-benzimidazolyl)methyl]benzamide (12b). Synthesized according to General Procedure B from **11b** (104 mg, 337 μmol); off-white powder after lyophilization (23 mg, 22%). ^{1}H NMR (400 MHz, DMSO-d_6): δ 11.16 (br s, 1H), 9.02 (br s, 1H), 7.69, 7.11 (AA′XX′ multiplet, $J_{AX} + J_{AX'}$ = 8.2 Hz, 4H), 7.64−7.58 (m, 1H), 7.43−7.38 (m, 1H), 7.19−7.13 (m, 2H), 5.58 (s, 2H), 3.26 (septuplet, J = 6.7 Hz, 1H), 1.25 (d, J = 6.4 Hz, 6H). ^{13}C NMR (100 MHz, DMSO-d_6): δ 163.8, 159.8, 142.2, 140.4, 135.1, 131.9, 127.3 (2C), 126.2 (2C), 121.7, 121.4, 118.6, 110.2, 45.5, 25.7, 21.7 (2C). ESI HRMS calcd. for C$_{18}$H$_{20}$F$_2$N$_3$O$_2$: [M + H]$^+$, m/z 310.1550. Found: 310.1554.

N-Hydroxy-4-[[2-(trifluoromethyl)-1-benzimidazolyl]methyl]-benzamide (12c). Synthesized according to General Procedure B from **11c** (295 mg, 882 μmol); off-white powder after lyophilization (51 mg, 16%). ^{1}H NMR (400 MHz, DMSO-d_6): δ 11.2 (br s, 1H), 7.89 (d, J = 7.8 Hz, 1H), 7.70, 7.14 (AA′XX′ multiplet, $J_{AX} + J_{AX'}$ = 8.1 Hz, 4H), 7.68 (partially concealed d, 1H), 7.48−7.38 (m, 2H), 5.77 (s, 2H). ^{13}C NMR (100 MHz, DMSO-d_6): δ 163.6, 140.5, 139.6 (q, J = 38 Hz), 138.9, 135.6, 132.3, 127.4 (2C), 126.0 (2C), 125.7, 123.8, 121.0, 119.0 (q, J = 270 Hz), 112.0, 47.3. ESI HRMS calcd. for C$_{16}$H$_{11}$F$_3$N$_3$O$_2$: [M − H]$^+$, m/z 334.0809. Found: 334.0802.

4-[[2-(3-Acetamidopropyl)-1-benzimidazolyl]methyl]-N-hydroxy-benzamide (12d). Synthesized according to General Procedure B from **11d** (88 mg, 261 μmol); off-white powder after lyophilization (53 mg, 60%). ^{1}H NMR (400 MHz, CD$_3$OD): δ 7.71 (d, J = 8.2 Hz, 2H), 7.62 (dd, J = 6.1, 2.6 Hz, 1H), 7.38 (dd, J = 6.1, 2.7 Hz, 1H), 7.28−7.18 (m, 2H), 7.07 (d, J = 8.3 Hz, 2H), 5.51 (s, 2H), 3.24 (t, J = 6.9 Hz, 2H), 2.91 (t, J = 7.7 Hz, 2H), 1.99−1.92 (m, 2H), 1.90 (s, 3H). ^{13}C NMR (100 MHz, CD$_3$OD): δ 173.3, 166.2, 156.3, 143.2, 143.0, 138.8, 136.5, 128.0 (2C), 127.1 (2C), 123.8, 123.5, 119.2, 111.3, 47.6, 39.9, 28.3, 25.6, 22.6. ESI HRMS calcd. for C$_{20}$H$_{21}$N$_4$O$_3$: [M − H]$^+$, m/z 365.1619. Found: 365.1625.

4-[[2-[2-(Dimethylamino)ethyl]-1-benzimidazolyl]methyl]-N-hy-droxybenzamide (12e). Synthesized according to General Procedure B from **11e** (53 mg, 145 μmol); off-white powder after lyophilization (36 mg, 68%). ^{1}H NMR (400 MHz, DMSO-d_6): δ 7.69 (A part of an AA′XX′ multiplet, $J_{AX} + J_{AX'}$ = 8.2 Hz, 2H), 7.58 (m, 1H), 7.43 (m, 1H), 7.18−7.12 (m, 4H), 5.56 (s, 2H), 2.97 (t, J = 7.6 Hz, 2H), 2.65 (t, J = 7.6

Hz, 2H), 2.13 (s, 6H). ^{13}C NMR (100 MHz, DMSO-d_6): δ 163.6, 153.9, 142.3, 139.8, 135.2, 132.5, 127.1 (2C), 126.3 (2C), 121.7, 121.4, 118.4, 110.1, 56.7, 45.8, 44.9 (2C), 25.1. ESI HRMS calcd. for C$_{19}$H$_{21}$N$_4$O$_2$: [M − H]$^+$, m/z 337.1670. Found: 337.1672.

tert-Butyl 4-[4-(Methoxycarbonyl)benzyl]-3,4-dihydroquinoxa-line-1(2H)-carboxylate (16a). Synthesized according to General Procedure A from **15a** (90 mg, 0.38 mmol), **10** (117 mg, 0.51 mmol), and K$_2$CO$_3$ (105 mg, 0.76 mmol); off-white waxy solid (90 mg, 60%). ^{1}H NMR (400 MHz, CDCl$_3$): δ 7.99, 7.32 (AA′XX′ multiplet, $J_{AX} + J_{AX'}$ = 8.2 Hz, 4H), 7.48 (br d, J = 7.4 Hz, 1H), 6.90 (td, J = 7.8 Hz, 1.1 Hz, 1H), 6.66 (td, J = 7.6 Hz, 1.2 Hz, 1H), 6.55 (dd, J = 8.2 Hz, 0.9 Hz, 1H), 4.56 (s, 2H), 3.90 (s, 3H), 3.88−3.84 (m, 2H), 3.46−3.43 (m, 2H), 1.53 (s, 9H). ^{13}C NMR (100 MHz, DMSO-d_6): δ 166.9, 153.3, 143.7, 138.2, 130.1 (2C), 129.1, 126.5 (2C), 125.1, 124.7, 116.3, 111.6, 100.0, 81.1, 54.9, 52.1, 49.5, 41.6, 28.4 (3C). ESI LRMS: [M + H]$^+$, m/z 383.3.

Methyl 4-[[2,3-Dihydro-4H-benzo[b][1,4]thiazin-4-yl)]methyl]-benzoate (16b). Synthesized according to General Procedure A from **15b** (230 mg, 1.52 mmol), **10** (513 mg, 2.25 mmol), and K$_2$CO$_3$ (420 mg, 3.04 mmol); colorless oil (360 mg, 80%). ^{1}H NMR (400 MHz, CDCl$_3$): δ 8.00, 7.33 (AA′XX′ multiplet, $J_{AX} + J_{AX'}$ = 8.4 Hz, 4H), 7.08 (dd, J = 7.7 Hz, 1.5 Hz, 1H), 6.90 (td, J = 7.8 Hz, 1.1 Hz, 1H), 6.63 (td, J = 7.5 Hz, 0.8 Hz, 1H), 6.54 (dd, J = 8.3 Hz, 0.7 Hz, 1H), 4.57 (s, 2H), 3.90 (s, 3H), 3.70−3.67 (m, 2H), 3.09−3.07 (m, 2H). ^{13}C NMR (100 MHz, CDCl$_3$): δ 166.9, 143.8, 143.4, 130.1 (2C), 129.1, 128.0, 126.6 (2C), 126.1, 118.0, 117.8, 113.2, 56.3, 52.1, 50.6, 25.9. ESI LRMS: [M + H]$^+$, m/z 300.2.

tert-Butyl 4-[4-(Methoxycarbonyl)benzyl]-3-oxo-3,4-dihydroqui-noxaline-1(2H)-carboxylate (19). To a round-bottom flask charged with NaH (60 weight% in mineral oil, 24 mg, 0.60 mmol) suspended in DMF (1 mL) was added **18**[32] (124 mg, 0.50 mmol) as a solution in DMF (1 mL) under an atmosphere of argon. After 30 min, a DMF solution (1 mL) of **10** (114 mg, 0.5 mmol) was added, and the resulting solution was allowed to stir overnight. The reaction was quenched by the addition of water (15 mL), and the organics were extracted with EtOAc (3 × 10 mL). The combined organic layers were washed with copious volumes of water and with brine, and dried over sodium sulfate. The evaporation residue was purified by flash chromatography (0−50% EtOAc/hexanes) to afford the title compound as a yellow oil (151 mg, 89%). ^{1}H NMR (400 MHz, CDCl$_3$): δ 7.99, 7.27 (AA′XX′ multiplet, $J_{AX} + J_{AX'}$ = 8.1 Hz, 4H), 7.65 (br d, J = 6.7 Hz, 1H), 7.06 (m, 1H), 7.01 (m, 1H), 6.83 (d, J = 8.0 Hz, 1H), 5.19 (s, 2H), 4.52 (s, 2H), 3.89 (s, 3H), 1.55 (s, 9H). ^{13}C NMR (100 MHz, CDCl$_3$): δ 166.7, 166.6, 152.1, 141.5, 132.5, 130.2 (2C), 129.4, 128.7, 126.3 (2C), 125.3, 124.2, 123.4, 115.9, 82.5, 52.1, 48.0, 46.2, 28.2 (3C). ESI LRMS: [M + H]$^+$, m/z 397.2.

4-[[1,2,3,4-Tetrahydroquinoxalin-1-yl]methyl]-N-hydroxybenza-mide (17a). The title compound was prepared according to a modified version of General Procedure B starting from **16a** (104 mg, 0.27 mmol). The reaction was quenched as above, and after neutralization to pH 7 the product was extracted into EtOAc (2 × 10 mL). The combined organic phases were washed with brine, dried over sodium sulfate, and concentrated under vacuum. The crude material was dissolved in DCM (2 mL). TFA (1 mL) was added, and the solution was allowed to stir 30 min before again being concentrated. The residue was purified by preparative HPLC, neutralized, and lyophilized to afford the title compound as an off-white powder (28 mg, 37% over 2 steps). ^{1}H NMR (400 MHz, DMSO-d_6): δ 11.15 (s, 1H), 8.99 (s, 1H), 7.70 (d, J = 8.1 Hz, 2H), 7.34 (d, J = 8.0 Hz, 2H), 6.57−6.16 (m, 4H), 5.48 (br s, 1H), 4.43 (s, 2H), 3.34 (s, 4H). ^{13}C NMR (100 MHz, DMSO-d_6): δ 164.2, 142.6, 135.0, 134.1, 131.3, 127.0 (2C), 126.9 (2C), 117.3, 117.0, 113.1, 111.2, 54.2, 48.2, 40.1. ESI HRMS calcd. for C$_{16}$H$_{16}$N$_3$O$_2$: [M − H]$^+$, m/z 282.1248. Found: 282.1248.

4-[[4-(Cyclopropylmethyl)-1,2,3,4-tetrahydroquinoxalin-1-yl]-methyl]-N-hydroxybenzamide (17b). To a round-bottom flask charged with **16a** (200 mg, 0.52 mmol) in DCM (2 mL) was added TFA (1 mL), and the resulting solution was allowed to stir for 30 min. The excess acid and solvent were removed under vacuum. The crude product was neutralized with saturated aqueous sodium carbonate and extracted with EtOAc (3 × 10 mL). The combined organic layers were washed with copious volumes of water and with brine, dried over sodium sulfate, and concentrated under vacuum. The deprotected product (120

mg, 0.42 mmol) was dissolved in DMF (3 mL), and K$_2$CO$_3$ (116 mg, 0.84 mmol) and (bromomethyl)cyclopropane (84 mg, 0.63 mmol) were added. The resulting mixture was heated at 80 °C for 2 h. Then the reaction was quenched by the addition of water (15 mL), and the organics were extracted with EtOAc (3 × 10 mL). The combined organic layers were washed with copious volumes of water and with brine, dried over sodium sulfate, and concentrated under vacuum. The crude benzoate intermediate was obtained (130 mg, 0.40 mmol) as light yellow oil. The title compound was prepared according to General Procedure B from the benzoate intermediate (130 mg, 0.40 mmol) and purified by preparative HPLC; off-white powder after neutralization and lyophilization (60 mg, 18% over three steps). ^{1}H NMR (400 MHz, DMSO-d_6): δ 11.15 (s, 1H), 8.99 (s, 1H), 7.70 (d, J = 8.0 Hz, 2H), 7.33 (d, J = 8.0 Hz, 2H), 6.58 (d, J = 7.8 Hz, 1H), 6.49 (t, J = 7.5 Hz, 1H), 6.40 (t, J = 7.4 Hz, 1H), 6.34 (d, J = 7.0 Hz, 1H), 4.45 (s, 2H), 3.42 (s, 4H), 3.09 (d, J = 6.4 Hz, 2H), 1.07−0.93 (m, 1H), 0.48 (q, J = 4.9 Hz, 2H), 0.23 (q, J = 4.9 Hz, 2H). ^{13}C NMR (100 MHz, DMSO-d_6): δ 164.2, 142.4, 135.2, 135.1, 131.3, 127.1 (2C), 126.8 (2C), 117.4, 117.3, 111.0, 110.9, 54.8, 54.4, 48.1, 46.5, 7.7, 3.4 (2C). ESI HRMS calcd. for C$_{20}$H$_{22}$N$_3$O$_2$: [M − H]$^+$, m/z 336.1718. Found: 336.1710.

4-[[2,3-Dihydro-4H-benzo[b][1,4]thiazin-4-yl]methyl]-N-hydroxy-benzamide (17c). Synthesized according to General Procedure B from **16b** (211 mg, 0.71 mmol) and purified via preparative HPLC; off-white powder after neutralization and lyophilization (19 mg, 9%). ^{1}H NMR (400 MHz, DMSO-d_6): δ 11.17 (s, 1H), 9.01 (s, 1H), 7.72 (d, J = 8.1 Hz, 2H), 7.32 (d, J = 8.1 Hz, 2H), 6.97 (dd, J = 7.9, 1.2 Hz, 1H), 6.83 (t, J = 7.7 Hz, 1H), 6.53 (t, J = 7.0 Hz, 2H), 3.78−3.55 (m, 2H), 3.20−2.99 (m, 2H). ^{13}C NMR (100 MHz, DMSO-d_6): δ 164.1, 143.0, 142.0, 131.4, 127.4, 127.2 (2C), 126.5 (2C), 125.8, 116.9, 116.9, 112.8, 55.0, 50.4, 25.0. ESI HRMS calcd. for C$_{16}$H$_{15}$N$_2$O$_2$S: [M − H]$^+$, m/z 299.0860. Found: 299.0877.

N-Hydroxy-4-[[1-oxido-2,3-dihydro-4H-benzo[b][1,4]thiazin-4-yl]methyl]benzamide (17d). Obtained as a side product from the synthesis of **17c** that elutes 8 min earlier during preparative HPLC. After neutralization and lyophilization, the title compound was obtained as an off-white solid (20 mg, 9% with respect to **16b**). ^{1}H NMR (400 MHz, DMSO-d_6): δ 7.71 (d, J = 7.8 Hz, 2H), 7.50 (d, J = 7.4 Hz, 1H), 7.31 (d, J = 7.9 Hz, 2H), 7.26 (d, J = 7.8 Hz, 1H), 6.76 (d, J = 8.6 Hz, 1H), 6.68 (t, J = 7.1 Hz, 1H), 4.78 (dd, J = 46.2, 17.5 Hz, 2H), 3.99 (t, J = 13.9 Hz, 1H), 3.67 (d, J = 13.8 Hz, 1H), 3.14 (d, J = 12.1 Hz, 1H), 2.96 (t, J = 14.1 Hz, 1H). ^{13}C NMR (100 MHz, CD$_3$OD): δ 167.8, 144.7, 143.0, 135.6, 134.5, 132.5, 128.6 (2C), 127.7 (2C), 121.7, 117.5, 115.1, 56.3, 42.3, 39.6. ESI HRMS calcd. for C$_{16}$H$_{15}$N$_2$O$_3$S: [M − H]$^+$, m/z 315.0809. Found: 315.0801.

tert-Butyl 4-[4-(Hydroxycarbamoyl)benzyl]-3-oxo-3,4-dihydro-quinoxaline-1(2H)-carboxylate (17e). Synthesized according to General Procedure B from **19** (156 mg, 0.39 mmol) and purified by preparative HPLC; off-white powder after neutralization and lyophilization (47 mg, 31%). ^{1}H NMR (400 MHz, CD$_3$OD): δ 7.74, 7.30 (AA′XX′ multiplet, J_{AX} + $J_{AX'}$ = 8.2 Hz, 4H), 7.63 (m, 1H), 7.16−7.04 (m, 3H), 5.31 (s, 2H), 4.53 (s, 2H), 1.57 (s, 9H). ^{13}C NMR (100 MHz, DMSO-d_6): δ 166.2, 163.9, 151.7, 139.8, 132.3, 131.7, 128.3, 127.2 (2C), 126.2 (2C), 125.3, 124.3, 122.8, 116.0, 81.6, 47.2, 44.6, 27.7 (3C). ESI HRMS calcd. for C$_{21}$H$_{22}$N$_3$O$_5$: [M − H]$^+$, m/z 396.1565. Found: 396.1564.

N-Hydroxy-4-[(2-oxoquinoxalin-1(2H)-yl)methyl]benzamide TFA Salt (17f). To a round-bottom flask charged with **17e** (45 mg, 0.118 mmol) in DCM (0.5 mL) was added TFA (0.5 mL), and the resulting solution was allowed to stir for 30 min. The solution was concentrated, and the residue was purified by preparative HPLC to afford the title compound as an off-white powder after lyophilization as its TFA salt (28 mg, 58%). ^{1}H NMR (400 MHz, DMSO-d_6): δ 11.17 (s, 1H), 9.0 (br s, 1H), 8.37 (s, 1H), 7.87 (d, J = 7.9 Hz, 1H), 7.69, 7.34 (AA′XX′ multiplet, J_{AX} + $J_{AX'}$ = 8.2 Hz, 4H), 7.56 (m, 1H), 7.43 (d, J = 8.4 Hz, 1H), 7.37 (m, 1H), 5.53 (s, 2H). ^{13}C NMR (100 MHz, CD$_3$OD): δ 168.0, 157.1, 151.3, 140.9, 135.2, 133.9, 133.3, 132.8, 131.6, 128.9 (2C), 128.4 (2C), 125.6, 116.6, 46.4. ESI HRMS calcd. for C$_{16}$H$_{12}$N$_3$O$_3$: [M − H]$^+$, m/z 294.0884. Found: 294.0880.

Methyl 2-(Chloromethyl)oxazole-4-carboxylate (21a). Synthesized according to a published procedure; all spectral data are in agreement with the published report.[20]

Methyl 2-(Chloromethyl)thiazole-4-carboxylate (21b). Synthesized according to a published procedure; all spectral data are in agreement with the published report.[20]

Methyl 6-(Bromomethyl)nicotinate (21c). Synthesized according to a published procedure; all spectral data are in agreement with the published report.[33]

Methyl 4-(Bromomethyl)-3-fluorobenzoate (21d). Synthesized from methyl 3-fluoro-4-methylbenzoate according to a published procedure;[34] purified by flash chromatography (0−10% EtOAc/hexanes); white waxy solid (345 mg, 61%). Spectral data match those published. ^{1}H NMR (400 MHz, CDCl$_3$): δ 7.81 (d, J = 7.9 Hz, 1H), 7.73 (d, J = 10.2 Hz, 1H), 7.47 (t, J = 7.6 Hz, 1H), 4.52 (s, 2H), 3.93 (s, 3H). ^{13}C NMR (100 MHz, CDCl$_3$): δ 165.5 (d, J = 2.9 Hz), 160.2 (d, J = 249 Hz), 132.5 (d, J = 7.7 Hz), 131.2 (d, J = 3.0 Hz), 130.1 (d, J = 14.7 Hz), 125.6 (d, J = 3.6 Hz), 116.9 (d, J = 23 Hz), 52.5, 24.5 (d, J = 4.2 Hz). ESI LRMS: [M + H]$^+$, m/z 247.0.

Methyl 2-[(2-Methyl-1-benzimidazolyl)methyl]oxazole-4-carboxylate (22a). Synthesized according to General Procedure A from **21a** (500 mg, 2.85 mmol) and purified by flash chromatography (0−5% MeOH/DCM); off-white waxy solid (556 mg, 72%). ^{1}H NMR (400 MHz, CDCl$_3$): δ 8.13 (s, 1H), 7.68 (m, 1H), 7.42 (m, 1H), 7.28−7.22 (m, 2H), 5.41 (s, 2H), 3.91 (s, 3H), 2.71 (s, 3H). ^{13}C NMR (100 MHz, CDCl$_3$): δ 160.9, 159.0, 151.3, 145.0, 142.5, 134.8, 133.6, 122.8, 122.5, 119.3, 109.0, 52.3, 40.4, 13.9. ESI LRMS: [M + H]$^+$, m/z 273.1.

Methyl 2-[(2-Methyl-1-benzimidazolyl)methyl]thiazole-4-carboxylate (22b). Synthesized according to General Procedure A from **21b** (225 mg, 1.17 mmol) and purified by flash chromatography (0−5% MeOH/DCM); off-white waxy solid (171 mg, 51%). ^{1}H NMR (400 MHz, CDCl$_3$): δ 8.09 (s, 1H), 7.72 (m, 1H), 7.31−7.21 (m, 3H), 5.63 (s, 2H), 3.96 (s, 3H), 2.64 (s, 3H). ^{13}C NMR (100 MHz, CDCl$_3$): δ 166.9, 161.3, 151.2, 147.1, 142.7, 134.5, 128.4, 122.9, 122.7, 119.5, 108.9, 52.6, 45.3, 13.9. ESI LRMS: [M + H]$^+$, m/z 288.1.

Methyl 6-[(2-Methyl-1-benzimidazolyl)methyl]nicotinate (22c). Synthesized according to General Procedure A from **21c** (181 mg, 0.79 mmol) and purified by flash chromatography (0−5% MeOH/DCM); viscous orange oil (143 mg, 72%). ^{1}H NMR (400 MHz, CDCl$_3$): δ 9.20 (s, 1H), 8.16 (dd, J = 8.0, 2.0 Hz, 1H), 7.74 (d, J = 7.6 Hz, 1H), 7.28−7.71 (m, 3H), 6.79 (d, J = 8.4 Hz, 1H), 5.49 (s, 2H), 3.93 (s, 3H), 2.60 (s, 3H). ^{13}C NMR (100 MHz, CDCl$_3$): δ 165.2, 160.0, 151.8, 151.0, 142.7, 138.4, 135.1, 125.3, 122.5, 122.3, 119.9, 119.3, 109.0, 52.4, 48.9, 13.9. ESI LRMS: [M + H]$^+$ m/z 282.1.

Methyl 3-Fluoro-4-[(2-methyl-1-benzimidazolyl)methyl]benzoate (22d). Synthesized according to General Procedure A from **21d** (170 mg, 0.69 mmol) and purified by flash chromatography (0−5% MeOH/DCM); viscous orange oil (145 mg, 71%). ^{1}H NMR (400 MHz, CDCl$_3$): δ 7.81−7.67 (m, 3H), 7.29−7.19 (m, 3H), 6.75 (t, J = 7.8 Hz, 1H), 5.40 (s, 2H), 3.90 (s, 3H), 2.58 (s, 3H). ^{13}C NMR (100 MHz, CDCl$_3$): δ 165.4 (d, J = 2.8 Hz), 159.7 (d, J = 247 Hz), 151.7, 142.6, 135.1, 132.0 (d, J = 7.6 Hz), 128.0 (d, J = 14.5 Hz), 127.8 (d, J = 3.7 Hz), 125.8 (d, J = 3.5 Hz), 122.6, 122.4, 119.3, 116.7 (d, J = 22.9 Hz), 109.1, 52.5, 41.1 (d, J = 5.0 Hz), 13.8. ESI LRMS: [M + H]$^+$, m/z 299.1.

Methyl 3-Fluoro-4-[(2-(trifluoromethyl)-1-benzimidazolyl)methyl]benzoate (22e). Synthesized according to General Procedure A from **21d** (97 mg, 0.39 mmol) and **9c** (73 mg, 0.39 mmol) and purified by flash chromatography (0−40% EtOAc/hexanes); yellow oil (104 mg, 75%). ^{1}H NMR (400 MHz, CDCl$_3$): δ 7.89 (m, 1H), 7.76 (dd, J = 10.5, 1.4 Hz, 1H), 7.65 (dd, J = 8.1, 1.1 Hz, 1H), 7.39−7.32 (m, 2H), 7.29−7.22 (m, 1H), 6.71 (t, J = 7.7 Hz, 1H), 5.60 (s, 2H), 3.86 (s, 3H). ^{13}C NMR (100 MHz, CDCl$_3$): δ 165.1 (d, J = 2.7 Hz), 159.4 (d, J = 247 Hz), 141.0, 140.7 (q, J = 39 Hz), 135.2, 132.2 (d, J = 7.6 Hz), 127.4 (d, J = 3 Hz), 127.0 (d, J = 14 Hz), 125.8, 125.7 (d, J = 3.5 Hz), 124.0, 121.8, 118.9 (q, J = 270 Hz), 116.6 (d, J = 23 Hz), 110.4, 52.3, 41.9 (m). ESI LRMS: [M + H]$^+$, m/z 353.1.

Methyl 4-(Bromomethyl)-2,3,5,6-tetrafluorobenzoate (25). To a round-bottom flask charged with methyl 2,3,5,6-tetrafluoro-4-methyl-benzoate (**24**, 1.00 g, 4.50 mmol) in CCl$_4$ (8 mL) were added N-bromosuccinimide (2.40 g, 13.5 mmol) and AIBN (74 mg, 0.45 mmol)

in succession. The resulting solution was allowed to stir at reflux temperature for 12 h under an atmosphere of Ar. The reaction mixture was concentrated under vacuum, and the residue was purified by flash chromatography (0−10% EtOAc/hexanes) to afford the title compound as a light yellow oil (1.1 g, 79%). ^{1}H NMR (400 MHz, CDCl$_3$): δ 4.51 (t, J = 1.3 Hz, 2H), 3.99 (s, 3H). ^{13}C NMR (100 MHz, CDCl$_3$): δ 159.9, approximately 145.8 and approximately 143.3 (together forming m, 4C), 120.1 (t, J = 16.4 Hz), 112.9 (t, J = 15.6 Hz), 53.4, 15.7. ESI LRMS: [M + H]$^+$, m/z 301.0.

Methyl 2,3,5,6-Tetrafluoro-4-[(2-methyl-1-benzimidazolyl)-methyl]benzoate (22f). Synthesized according to General Procedure A from **25** (1.10 g, 3.7 mmol) and **9a** (537 mg, 4.1 mmol) and purified by flash chromatography (0−10% MeOH/DCM); light yellow waxy solid (1.15 g, 88%). ^{1}H NMR (400 MHz, CDCl$_3$): δ 7.68 (m, 1H), 7.28−7.20 (m, 3H), 5.41 (s, 2H), 3.97 (s, 3H), 2.71 (s, 3H). ^{13}C NMR (100 MHz, CDCl$_3$): δ 159.5, 151.6, approximately 146 and approximately 143.5 (together forming m, 4C), 142.6, 134.6, 122.7, 122.5, 119.7, 117.1 (t, J = 16.3 Hz), 113.4, 108.8 (t, J = 2.4 Hz), 53.5, 36.1, 13.9. LRMS ESI [M + H]$^+$, m/z 353.1.

Ethyl 2,6-Difluoro-4-[[(tetrahydropyran-2-yl)oxy]methyl]-benzoate (27). To a round-bottom flask charged with 2-(3,5-difluorobenzyloxy)tetrahydropyran (**26**, 370 mg, 1.62 mmol) in THF (3 mL) under an atmosphere of argon was added n-BuLi (2.0 M in cyclohexane, 0.89 mL, 1.78 mmol) dropwise at −78 °C. Stirring was continued at this temperature while a solution of ethyl chloroformate (185 μL, 1.94 mmol) in THF (2 mL) was added; then the solution was allowed to slowly warm to room temperature. The reaction was monitored by TLC and quenched after 2 h with saturated aqueous ammonium chloride solution (5 mL). The organics were extracted into EtOAc (3 × 5 mL). The combined organic layers were washed with brine, dried over sodium sulfate, and evaporated. The crude product was purified by flash chromatography (0−20% EtOAc/hexanes) to afford the title compound as a light yellow oil (434 mg, 89%). ^{1}H NMR (400 MHz, CDCl$_3$): δ 6.96 (d, J = 8.8 Hz, 2H), 4.77 (d, J = 13.6 Hz, 1H), 4.70 (t, J = 3.2 Hz, 1H), 4.50 (d, J = 13.6 Hz, 1H), 4.41 (q, J = 7.0 Hz, 2H), 3.89−3.83 (m, 1H), 3.62−3.44 (m, 1H), 1.92−1.53 (m, 6H), 1.39 (t, J = 7.1 Hz, 3H). ^{13}C NMR (100 MHz, CDCl$_3$) δ 161.0 (dd, J = 257 Hz, 6.6 Hz, 2C), 161.6, 145.2 (t, J = 9.5 Hz), 110.4 and 110.2 (together forming m, 2C), 109.8 (t, J = 18.0 Hz), 98.1, 67.1, 62.2, 61.9, 30.4, 25.4, 19.2, 14.2. LRMS ESI [M + H]$^+$, m/z 301.1

Ethyl 2,6-Difluoro-4-[(2-methyl-1-benzimidazolyl)methyl]-benzoate (22g). To a round-bottom flask charged with **27** (275 mg, 0.92 mmol) in methanol (5 mL) was added p-TsOH·H$_2$O (17 mg, 92 μmol). The resulting solution was allowed to stir for 1 h at room temperature, then concentrated under vacuum. The residue was taken up in saturated aqueous sodium bicarbonate solution (5 mL), and the alcohol intermediate was extracted into EtOAc (3 × 5 mL). The combined organic layers were washed with brine, dried over sodium sulfate, and concentrated to dryness. The residue was dissolved in DCM (5 mL). Triethylamine (255 μL, 1.83 mmol) and mesyl chloride (85 μL, 1.10 mmol) were added sequentially, and the mixture was allowed to stir at room temperature for 1 h. Upon completion of the reaction, as judged by TLC, the solution was washed with 0.1 M HCl, dried over sodium sulfate, and concentrated under vacuum. The crude mesylate was taken up in DMF (2 mL), and to the solution were added sequentially **9a** (145 mg, 1.1 mmol) and K$_2$CO$_3$ (253 mg, 1.83 mmol). The mixture was stirred for 2 h at 80 °C. The reaction was quenched with water and worked up in the usual manner. The crude product was purified by flash chromatography (0−5% MeOH/DCM) to afford the title compound as a light yellow oil (35 mg, 12% over three steps). ^{1}H NMR (400 MHz, CDCl$_3$): δ 7.75 (d, J = 7.6 Hz, 1H), 7.28 (m, 1H), 7.23 (m, 1H), 7.14 (br d, J = 7.5 Hz, 1H), 6.62 (A part of an AA′XX′ multiplet [X being fluorine], J_{AX} + $J_{AX'}$ = 8.2 Hz, 2H), 5.31 (s, 2H), 4.39 (q, J = 7.1 Hz, 2H), 2.56 (s, 3H), 1.36 (t, J = 7.1 Hz, 3H). ^{13}C NMR (100 MHz, CDCl$_3$): δ 161.0 (dd, J = 257 Hz, 6.6 Hz, 2C), 160.9, 151.4, 142.6, 142.0 (t, J = 9.0 Hz), 134.9, 122.6 (d, J = 24 Hz, 2C), 119.5, 110.9 (t, J = 18.0 Hz), 109.8 and 109.6 (together forming m, 2C), 108.9, 62.1, 46.1, 14.1, 13.8. ESI LRMS: [M + H]$^+$, m/z 317.1.

N-Hydroxy-2-[(2-methyl-1-benzimidazolyl)methyl]oxazole-4-car-boxamide (23a). Synthesized according to General Procedure B from **22a** (338 mg, 1.24 mmol) and purified by preparative HPLC; off-white powder after lyophilization (61 mg, 18%). ^{1}H NMR (400 MHz, DMSO-d_6): δ 11.12 (br s, 1H), 9.12 (br s, 1H), 8.57 (s, 1H), 7.58−7.56 (m, 2H), 7.26−7.19 (m, 2H), 5.74 (s, 2H), 2.62 (s, 3H). ^{13}C NMR (100 MHz, DMSO-d_6): δ 159.0, 157.4, 152.1, 142.2, 140.8, 134.7, 134.7, 122.4, 122.2, 117.8, 110.1, 40.1, 13.3. ESI HRMS calcd. for C$_{13}$H$_{11}$N$_4$O$_3$: [M − H]$^+$, m/z 271.0837. Found: 271.0834.

N-Hydroxy-2-[(2-methyl-1-benzimidazolyl)methyl]thiazole-4-car-boxamide (23b). Synthesized according to General Procedure B from **22b** (171 mg, 0.60 mmol) and purified by preparative HPLC; off-white powder after lyophilization (140 mg, 68%). ^{1}H NMR (400 MHz, DMSO-d_6): δ 11.11 (br s, 1H), 9.12 (br s, 1H), 8.26 (s, 1H), 7.93 (m, 1H), 7.78 (m, 1H), 7.51−7.49 (m, 2H), 6.09 (s, 2H), 2.94 (s, 3H). ^{13}C NMR (100 MHz, DMSO-d_6): δ 162.4, 157.9, 152.7, 148.4, 131.5, 130.1, 126.0, 125.6, 125.4, 114.1, 112.6, 44.3, 12.0. ESI HRMS calcd. for C$_{13}$H$_{13}$N$_4$O$_2$S: [M + H]$^+$, m/z 289.0754. Found: 289.0768.

N-Hydroxy-6-[(2-methyl-1-benzimidazolyl)methyl]nicotinamide (23c). Synthesized according to General Procedure B from **22c** (143 mg, 0.51 mmol); off-white powder after neutralization and lyophilization (80 mg, 56%). ^{1}H NMR (400 MHz, DMSO-d_6): δ 11.32 (br s, 1H), 9.20 (br s, 1H), 8.97 (s, 1H), 8.07 (d, J = 7.2 Hz, 1H), 7.54 (m, 1H), 7.43 (m, 1H), 7.29 (d, J = 8.1 Hz, 1H), 7.16−7.10 (m, 2H), 5.60 (s, 2H), 2.55 (s, 3H). ^{13}C NMR (100 MHz, DMSO-d_6): δ 162.3, 158.6, 152.3, 147.8, 142.4, 135.9, 135.3, 127.6, 121.6, 121.3, 121.2, 118.2, 109.9, 47.8, 13.7. ESI HRMS calcd. for C$_{15}$H$_{13}$N$_4$O$_2$: [M − H]$^+$, m/z 281.1044. Found: 281.1044.

3-Fluoro-N-hydroxy-4-[(2-methyl-1-benzimidazolyl)methyl]-benzamide (23d). Synthesized according to General Procedure B from **22d** (145 mg, 0.49 mmol); off-white powder after neutralization and lyophilization (72 mg, 50%). ^{1}H NMR (400 MHz, DMSO-d_6): δ 11.5 (br s, 1H), 7.85−7.79 (m, 2H), 7.67−7.60 (m, 2H), 7.58−7.50 (m, 2H), 7.46 (m, 1H), 5.85 (s, 2H), 2.89 (s, 3H). ^{13}C NMR (100 MHz, DMSO-d_6): δ 161.9, 159.8 (d, J = 246 Hz), 152.1, 135.1 (d, J = 7.2 Hz), 131.7, 130.1, 129.9 (d, J = 3.3 Hz), 125.9, 125.5, 124.1 (d, J = 14.3 Hz), 123.3 (d, J = 2.6 Hz), 114.2 (d, J = 23 Hz), 114.1, 112.7, 42.5 (d, J = 2.9 Hz), 11.7 (d, J = 1.4 Hz). ESI HRMS calcd. for C$_{16}$H$_{13}$FN$_3$O$_2$: [M − H]$^+$, m/z 298.0997. Found: 298.0998.

3-Fluoro-N-hydroxy-4-[(2-(trifluoromethyl)-1-benzimidazolyl)-methyl]benzamide (23e). Synthesized according to General Procedure B from **22e** (85 mg, 0.25 mmol); off-white powder after neutralization and lyophilization (79 mg, 93%). ^{1}H NMR (400 MHz, DMSO-d_6): δ 11.30 (s, 1H), 9.16 (s, 1H), 7.89 (d, J = 7.8 Hz, 1H), 7.70 (d, J = 7.9 Hz, 1H), 7.60 (d, J = 11 Hz, 1H), 7.53−7.39 (m, 3H), 6.91 (t, J = 7.7 Hz, 1H), 5.81 (s, 2H). ^{13}C NMR (100 MHz, DMSO-d_6): δ 162.3, 159.2 (d, J = 245 Hz), 140.4, 139.6 (d, J = 38 Hz), 135.6, 134.7 (d, J = 5 Hz), 128.1, 126.0/125.7 (presumably s overlapping with narrow d), 123.9, 123.4, 121.0, 118.9 (q, J = 271 Hz), 114.1 (d, J = 23 Hz), 111.8, 42.3. ESI HRMS calcd. for C$_{16}$H$_{10}$F$_4$N$_3$O$_2$: [M − H]$^+$, m/z 352.0715. Found: 352.0707.

2,3,5,6-Tetrafluoro-N-hydroxy-4-[(2-methyl-1-benzimidazolyl)-methyl]benzamide (23f). Synthesized according to General Procedure B from **22f** (500 mg, 1.40 mmol); off-white powder after neutralization and lyophilization (126 mg, 26%). ^{1}H NMR (400 MHz, DMSO-d_6): δ 11.36 (br s, 1H), 9.68 (br s, 1H), 7.54 (d, J = 7.4 Hz, 1H), 7.38 (d, J = 7.8 Hz, 1H), 7.23−7.13 (m, 2H), 5.66 (s, 2H), 2.57 (s, 3H). ^{13}C NMR (100 MHz, DMSO-d_6): δ 153.8, 152.1, 144.3 (m, 2C), 142.9 (m, 2C), 142.1, 134.9, 122.0, 121.7, 118.5, 116.5 (t, J = 15.6 Hz), 115.2 (t, J = 21 Hz), 109.4, 35.9, 13.5. ESI HRMS calcd. for C$_{16}$H$_{10}$F$_4$N$_3$O$_2$: [M − H]$^+$, m/z 352.0715. Found: 352.0721.

2,6-Difluoro-N-hydroxy-4-[(2-methyl-1-benzimidazolyl)methyl]-benzamide (23g). Synthesized according to General Procedure B from **22g** (35 mg, 0.11 mmol); off-white powder after neutralization and lyophilization (10 mg, 28%). ^{1}H NMR (400 MHz, DMSO-d_6): δ 11.14 (s, 1H), 9.43 (s, 1H), 7.57 (dd, J = 5.7 Hz, 3.2 Hz, 1H), 7.44 (dd, J = 5.9 Hz, 3.2 Hz, 1H), 7.28−7.09 (m, 2H), 6.89 (d, J = 8.0 Hz, 2H), 5.53 (s, 2H), 2.54 (s, 3H). ^{13}C NMR (100 MHz, DMSO-d_6): δ 159.0 (dd, J = 257 Hz, 6.6 Hz, 2C), 156.1, 152.0, 142.0 (overlapping), 142.0 (t, J = 9.0 Hz), 135.0, 121.9, 121.7, 118.4, 112.2 (t, J = 23.4 Hz), 110.2 and 110.1 (together forming m, 2C), 110.0, 45.4, 40.2, 13.5. ESI HRMS calcd. for C$_{16}$H$_{12}$F$_2$N$_3$O$_2$: [M − H]$^+$, m/z 316.0903. Found: 316.0906.

Methyl 4-[(6-Fluoro-2-methyl-1-benzimidazolyl)methyl]benzoate (29a). To a round-bottom flask charged with 4-fluoro-2-nitroacetanilide (28, 396 mg, 2.00 mmol) in MeOH (15 mL) under an atmosphere of argon was added Pd/C (10 weight%, 40 mg). A hydrogen atmosphere (balloon pressure) was established by three vacuum/purge cycles. The mixture was allowed to stir at room temperature overnight, then concentrated under vacuum to approximately one-third of its volume and filtered through a plug of Celite and concentrated. The crude aniline intermediate was taken up in 10% AcOH in DCE (10 mL), and methyl 4-formylbenzoate (328 mg, 2.00 mmol) and NaBH(OAc)$_3$ (636 mg, 3.00 mmol) were added sequentially under an atmosphere of argon. The resulting suspension was allowed to stir for 24 h at room temperature. The reaction was quenched with water (10 mL), and the solution was extracted with DCM (2 × 10 mL). The combined organic layers were washed with brine, dried over sodium sulfate, and concentrated. The crude reductive amination product was taken up in toluene (10 mL), and *p*-TsOH·H$_2$O (38 mg, 0.20 mmol) was added. The mixture was allowed to stir under reflux for 2 h. After cooling to room temperature, saturated aqueous sodium bicarbonate solution (10 mL) was added, and the organics were extracted into EtOAc (2 × 10 mL). The combined organic layers were washed with brine, dried over sodium sulfate, and concentrated under vacuum. Flash chromatography (0−10% MeOH/DCM) afforded the title compound as a light-yellow viscous oil (440 mg, 74% over 3 steps). ^{1}H NMR (400 MHz, CDCl$_3$): δ 7.99, 7.10 (AA′XX′ multiplet, $J_{AX} + J_{AX'}$ = 8.2 Hz, 4H), 7.64 (dd, J = 8.8 Hz, 4.8 Hz, 1H), 6.99 (td, J = 9.2, 2.4 Hz, 1H), 6.85 (dd, J = 8.5 Hz, 2.3 Hz, 1H), 5.32 (s, 2H), 3.90 (s, 3H), 2.55 (s, 3H). ^{13}C NMR (100 MHz, CDCl$_3$): δ 166.4, 159.6 (d, J = 238 Hz), 152.4 (d, J = 2.9 Hz), 140.4, 139.0, 135.4 (d, J = 12.8 Hz), 130.4 (2C), 130.1, 126.1 (2C), 120.0 (d, J = 9.9 Hz), 110.4 (d, J = 25 Hz), 96.2 (d, J = 28 Hz), 52.2, 47.1, 14.0. ESI LRMS: [M + H]$^+$, *m/z* 299.1.

Methyl 4-[(5-Fluoro-2-methyl-1-benzimidazolyl)methyl]benzoate (29b). To a round-bottom flask charged with 4-fluoro-2-nitroacetanilide (28, 872 mg, 4.4 mmol) in DMF (20 mL) were added 10 (1.0 g, 4.4 mmol) and K$_2$CO$_3$ (1.22 g, 8.8 mmol) sequentially. The mixture was allowed to stir at 80 °C for 1.5 h under an atmosphere of argon. The reaction was quenched with water (50 mL), and the organics were extracted into EtOAc (3 × 20 mL). The combined organic layers were washed with brine, dried over sodium sulfate, and concentrated under vacuum. The crude product (900 mg, 2.6 mmol) was used directly in the next step. To a stirred solution of the crude intermediate (350 mg, 1 mmol) in EtOH/AcOH (4/2.5 mL) was added iron powder at room temperature. The resulting mixture was refluxed for 4 h. Then the reaction was quenched with saturated aqueous sodium bicarbonate solution (20 mL), and the organics were extracted with EtOAc (3 × 15 mL). The combined organic layers were separated, washed with brine, dried over sodium sulfate, and concentrated under vacuum. The crude product was purified by flash chromatography (0−10% MeOH/DCM) to afford the title compound as a tan waxy solid (250 mg, 50% over 2 steps). ^{1}H NMR (400 MHz, CDCl$_3$): δ 7.99, 7.09 (AA′XX′ multiplet, $J_{AX} + J_{AX'}$ = 8.4 Hz, 2H), 7.40 (dd, J = 9.3 Hz, 2.4 Hz, 1H), 7.06 (dd, J = 8.8 Hz, 4.5 Hz, 1H), 6.94 (td, J = 9.1, 2.4 Hz, 1H), 5.35 (s, 2H), 3.90 (s, 3H), 2.56 (s, 3H). ^{13}C NMR (100 MHz, CDCl$_3$): δ 166.4, 159.4 (d, J = 236 Hz), 153.3, 143.2 (d, J = 12.5 Hz), 140.5, 131.8, 130.4 (2C), 130.1, 126.1 (2C), 110.6 (d, J = 26 Hz), 109.4 (d, J = 10.2 Hz), 105.3 (d, J = 24 Hz), 52.2, 47.1, 14.1. ESI LRMS: [M + H]$^+$, *m/z* 299.1.

4-[(6-Fluoro-2-methyl-1-benzimidazolyl)methyl]-N-hydroxybenzamide (30a). Synthesized according to General Procedure B from 29a (101 mg, 0.34 mmol); off-white powder after neutralization and lyophilization (13 mg, 13%). ^{1}H NMR (400 MHz, DMSO-d_6): δ 11.18 (s, 1H), 9.02 (s, 1H), 7.70, 7.18 (AA′XX′ multiplet, $J_{AX} + J_{AX'}$ = 8.1 Hz, 4H), 7.55 (dd, J = 8.7 Hz, 4.9 Hz, 1H), 7.39 (dd, J = 9.3 Hz, 2.2 Hz, 1H), 7.02−7.00 (m, 1H), 5.51 (s, 2H), 2.49 (s, 3H). ^{13}C NMR (100 MHz, DMSO-d_6): δ 163.9, 158.5 (d, J = 234 Hz), 152.9 (d, J = 2.7 Hz), 139.8, 138.8, 135.6 (d, J = 13.6 Hz), 132.2, 127.4 (2C), 126.6 (2C), 119.2 (d, J = 10.1 Hz), 109.3 (d, J = 25 Hz), 96.9 (d, J = 28 Hz), 46.1, 13.6. ESI HRMS calcd. for C$_{16}$H$_{13}$FN$_3$O$_2$: [M − H]$^+$, *m/z* 298.0997. Found: 298.0992.

4-[(5-Fluoro-2-methyl-1-benzimidazolyl)methyl]-N-hydroxybenzamide (30b). Synthesized according to General Procedure B from 29b

(41 mg, 0.14 mmol); off-white powder after neutralization and lyophilization (18 mg, 44%). ^{1}H NMR (400 MHz, DMSO-d_6): δ 11.16 (s, 1H), 9.01 (s, 1H), 7.69, 7.16 (AA′XX′ multiplet, $J_{AX} + J_{AX'}$ = 8.2 Hz, 4H), 7.45 (dd, J = 8.8 Hz, 4.7 Hz, 1H), 7.35 (dd, J = 9.8 Hz, 2.4 Hz, 1H), 7.01−7.00 (m, 1H), 5.52 (s, 2H), 2.51 (s, 3H). ^{13}C NMR (100 MHz, DMSO-d_6): δ 163.9, 158.4 (d, J = 232 Hz), 153.7, 142.7 (d, J = 12.7 Hz), 139.8, 132.1/131.9 (presumably s overlapping with d), 127.4 (2C), 126.6 (2C), 110.6 (d, J = 10.2 Hz), 109.5 (d, J = 25.5 Hz), 104.0 (d, J = 23.7 Hz), 46.1, 13.7. ESI HRMS calcd. for C$_{16}$H$_{13}$FN$_3$O$_2$: [M − H]$^+$, *m/z* 298.0997. Found: 298.0991.

Computational Methods. Docking simulations of HDAC6 and the benzimidazole derivatives were performed using the already published HDAC6 model[17] and AutoDock4.0 focusing the search on a 12 Å radius sphere around the Zn^{2+} ion. In detail, the resolution of the grid was 80 × 80 × 100 points with a grid spacing of 0.440 Å and each ligand was docked into this grid by the Lamarckian algorithm which ran 20 simulations per substrate with 2 000 000 energy evaluations and a maximum number of generations of 27 000. The crossover rate was equal to 0.8, and the number of individuals in each population was 150. All other parameters were left at the AutoDock default settings.[35] The best poses were selected considering both the scoring functions and the proximity of hydroxamate function to the Zn^{2+} ion and for almost all the analogues investigated, the best pose was also the lowest energy result, thus confirming the ability of AutoDock to suitably accommodate these compounds. The best complexes thus obtained were finally minimized keeping those atoms outside a 12 Å radius sphere surrounding the bound inhibitor fixed.

Cell Culture. Mouse neuroblastoma (N2a) cells were grown in a 1:1 mixture of DMEM (Dulbecco's modified Eagle's medium) and F12 medium supplemented with glutamax (ThermoFisher Scientific Inc., Pittsburgh, PA), 100 μg/mL streptomycin, 100 U/mL penicillin (ThermoFisher Scientific), 10% fetal calf serum (Greiner Bio-One, Alphen aan den Rijn, NL), 1% nonessential amino acids (ThermoFisher Scientific), and 1.6% NaHCO$_3$ (ThermoFisher Scientific) at 37 °C and 7.5% CO$_2$. To split the cells, cells were washed with Versene (ThermoFisher Scientific) and dissociated with 0.05% trypsin-EDTA (ThermoFisher Scientific). DRG neurons were cultured from 12 month old Thy1.2-HSPB1 S135F mice. The DRG neurons were dissected from the spinal cord and kept in cold Hibernate A (ThermoFisher Scientific) supplemented with B27 (ThermoFisher Scientific), further referred to as HA/B27. To extract the DRG neurons, the tissue was dissociated by a 45 min incubation of 2 mg/mL papain and thorough resuspension until all tissue was dissolved. The cell suspension was added to a gradient solution containing four layers of 37%, 25%, 20%, and 15% Optiprep (Sigma-Aldrich) in HA/B27 and centrifuged during 15 min at 800g without the brake. After centrifugation during 15 min at 800g, the cell suspension was washed in HA/B27. An additional centrifugation step was performed during 4 min at 400g, and the cells were plated in culture medium containing Neurobasal A (ThermoFisher Scientific) supplemented with B27 (ThermoFisher Scientific), 200 mM L-glutamine (ThermoFisher Scientific), 68 ng/mL NGF (Merck Millipore Corp, Darmstadt, Germany), and antibiotics. The N2a cells and DRG neurons were treated overnight at 37 °C with dosages ranging from 10 nM up to 1 μM of the compounds or an equivalent dose of DMSO (Sigma-Aldrich, Diegem, Belgium).

Western Blot Analysis. The treated cells were washed with phosphate-buffered saline (PBS) and collected using the EpiQuik Total Histone Extraction Kit (EpiGentek, Farmingdale, NY, USA) according to the manufacturer's instructions. Protein concentrations were determined using the microBCA kit (ThermoFisher Scientific) according to manufacturer's instructions. Before resolving the samples on a 12% sodium dodecyl sulfate−polyacrylamide gel electrophoresis (SDS-PAGE) gel, samples containing equal amounts of protein were supplemented with reducing sample buffer (Thermo Scientific) and heated at 95 °C for 5 min. After electrophoresis, the proteins were transferred to a polyvinylidene difluoride (PVDF) membrane (Merck Millipore Corp.). The nonspecific binding was blocked by incubation of the membrane in 5% bovine serum albumin (BSA), diluted in Tris Buffered Saline Tween (TBST, 50 mM TRIS, 150 mM NaCl, 0.1% Tween-20 (Applichem, Darmstadt, Germany)) for 1 h at room

temperature followed by incubation with primary antibodies overnight. The antibodies, diluted in TBS-T, were directed against α-tubulin (1/5000, T6199, Sigma-Aldrich), acetylated α-tubulin (1/5000, T6793 monoclonal, Sigma-Aldrich), histone H3 acetyl k9+k14 (1/1000, 9677L, Cell Signaling), and histone 4 (1/1000, ab10158, Abcam). The secondary antibodies, coupled to alkaline phosphatase (anti-mouse or anti-rabbit, 1/5000, Sigma-Aldrich), were used to detect the signal of the primary antibodies. Blots were visualized by adding the ECF substrate (Enhanced Chemical Fluorescence, GE Healthcare, Uppsala, Sweden) and imaged with the ImageQuant LAS 4000. A mild reblotting buffer (Merck Millipore Corp.) was applied to strip the blots. ImageQuant TL version 7.0 software was used to quantify the blots.

Genotyping of the Mice. Genotyping of the transgenic animals was done using KAPA Taq Ready Mix (Kapa Biosystems, Wilmington, MA, USA) and two sets of primers directed against the human cDNA of HSPB1 (forward primer 5′-CAgCTggCTgACCCTgTAgC-3′; reverse primer 5′-CTTggCggCAgTCTCATCg-3′) or directed against the mouse interleukin-2 gene, used as an internal control (forward primer 5′-CTAggCCACAgAATTGAAAgATCT-3′; reverse primer 5′-gTA-gTggAAATTCTAgCATCATCC-3′). All animals were housed under standard conditions according to the guidelines of the University of Leuven and bred to heterozygous state.

Axonal Transport Measurements. Prior to the measurements, the cultured DRG neurons were loaded with MitoTracker Red FM (50 nM, ThermoScientific). To visualize the mitochondria, the MitoTracker was excited at 580 nm by a TILL Poly V light source. During the measurements, the DRG neurons were perfused in HEPES solution (containing 148 mM NaCl, 5 mM KCl, 0.1 mM $MgCl_2 \cdot 1.6H_2O$, 10 mM glucose, 10 mM HEPES, and 2 mM $CaCl_2 \cdot 2.2H_2O$) at 37 °C via a heath-gravity fed perfusion system, and 200 images were recorded at 1 Hz with a cooled CCD camera using TILL VisION. To analyze different parameters of mitochondrial movement, kymographs or spatiotemporal maps were obtained by Igor Pro software (Wavemetrics) using custom-written routines based on a previous described analysis algorithm.

ASSOCIATED CONTENT

Ⓢ Supporting Information

The Supporting Information is available free of charge on the ACS Publications website at DOI: 10.1021/acschemneuro.5b00286.

> Complete ^{1}H and ^{13}NMR spectrum for all the intermediates and final compounds and supplementary figures for the molecular modeling and screening in N2a cells (PDF)

AUTHOR INFORMATION

Corresponding Authors

*(L.V.D.B.) E-mail: ludo.vandenbosch@vib-kuleuven.be. Phone: (+32)016 33 06 81.

*(A.P.K.) E-mail: kozikowa@uic.edu. Phone: 312-996-7577.

Author Contributions

‖S.S., V.B., and J.A.B. contributed equally to this work.

A.P.K. and L.V.D.B were responsible for the supervision and development of the entire project. S.S., V.B., and J.A.B. assembled the manuscript. S.S., J.A.B., J. H. K., and M.F. synthesized, purified, and characterized all the molecules presented in this paper. V.B. and W.H. assayed the compounds in the N2a cells and in the mutant HSPB1-expressing DRG neurons. G.V. was responsible for the modeling study.

Notes

The authors declare no competing financial interest.

ACKNOWLEDGMENTS

ABBREVIATIONS

CMT, Charcot−Marie−Tooth disease; SAR, structure activity relationships; HDAC, histone deacetylase; ZBG, zinc binding group; PTMs, post-translational modifications; HATs, histone acetyltransferases; TubaA, tubastatin A; SD, standard deviation; DRG, dorsal root ganglion; NTG, nontransgenic; N2a, neuro-2a; H4, histone 4; WB, Western blot; ADMET, absorption, distribution, metabolism, excretion, and toxicity; PK, pharmacokinetic; AUC, area under curve; DMF, dimethylformamide; THF, tetrahydrofuran; DCM, dichloromethane; DMSO, dimethyl sulfoxide; EDCI, 1-ethyl-3-(3-(dimethylamino)-propyl)carbodiimide; DMAP, 4-dimethylaminopyridine; TFA, trifluoroacetic acid; NBS, N-bromosuccinimide; AIBN, azobis-(isobutyronitrile); DMEM, dulbecco's modified eagle medium; EDTA, ethylenediaminetetraacetic acid; PBS, phosphate-buffered saline; SDS-PAGE, sodium dodecyl sulfate−polyacrylamide gel electrophoresis; PVDF, polyvinylidene difluoride; TBST, tris buffered saline Tween; ECF, enhanced chemical fluorescence; HEPES, 4-(2-hydroxyethyl)-1-piperazineethane-sulfonic acid

REFERENCES

(1) Barisic, N., Claeys, K. G., Sirotkovic-Skerlev, M., Lofgren, A., Nelis, E., De Jonghe, P., and Timmerman, V. (2008) Charcot-marie-tooth disease: A clinico-genetic confrontation. *Ann. Hum. Genet.* 72, 416−441.

(2) Zuchner, S., and Vance, J. M. (2006) Mechanisms of Disease: a molecular genetic update on hereditary axonal neuropathies. *Nat. Clin. Pract. Neurol.* 2, 45−53.

(3) d'Ydewalle, C., Krishnan, J., Chiheb, D. M., Van Damme, P., Irobi, J., Kozikowski, A. P., Vanden Berghe, P., Timmerman, V., Robberecht, W., and Van Den Bosch, L. (2011) HDAC6 inhibitors reverse axonal loss in a mouse model of mutant HSPB1-induced Charcot-Marie-Tooth disease. *Nat. Med.* 17, 968−986.

(4) Strahl, B. D., and Allis, C. D. (2000) The language of covalent histone modifications. *Nature* 403, 41−45.

(5) Altaf, M., Saksouk, N., and Cote, J. (2007) Histone modifications in response to DNA damage. *Mutat. Res., Fundam. Mol. Mech. Mutagen.* 618, 81−90.

(6) Liu, C. L., Tangsombatvisit, S., Rosenberg, J. M., Mandelbaum, G., Gillespie, E. C., Gozani, O. P., Alizadeh, A. A., and Utz, P. J. (2012) Specific post-translational histone modifications of neutrophil extracellular traps as immunogens and potential targets of lupus autoantibodies. *Arthritis Res. Ther.* 14, R25.

(7) Meaney, M. J., and Ferguson-Smith, A. C. (2010) Epigenetic regulation of the neural transcriptome: the meaning of the marks. *Nat. Neurosci.* 13, 1313−1318.

(8) Berger, S. L. (2007) The complex language of chromatin regulation during transcription. *Nature* 447, 407−412.

(9) Drummond, D. C., Noble, C. O., Kirpotin, D. B., Guo, Z., Scott, G. K., and Benz, C. C. (2005) Clinical development of histone deacetylase

inhibitors as anticancer agents. *Annu. Rev. Pharmacol. Toxicol. 45*, 495−528.

(10) Minucci, S., and Pelicci, P. G. (2006) Histone deacetylase inhibitors and the promise of epigenetic (and more) treatments for cancer. *Nat. Rev. Cancer 6*, 38−51.

(11) Li, J., Li, G., and Xu, W. (2013) Histone deacetylase inhibitors: an attractive strategy for cancer therapy. *Curr. Med. Chem. 20*, 1858−1886.

(12) Lane, A. A., and Chabner, B. A. (2009) Histone deacetylase inhibitors in cancer therapy. *J. Clin. Oncol. 27*, 5459−5468.

(13) Chuang, D. M., Leng, Y., Marinova, Z., Kim, H. J., and Chiu, C. T. (2009) Multiple roles of HDAC inhibition in neurodegenerative conditions. *Trends Neurosci. 32*, 591−601.

(14) Abel, T., and Zukin, R. S. (2008) Epigenetic targets of HDAC inhibition in neurodegenerative and psychiatric disorders. *Curr. Opin. Pharmacol. 8*, 57−64.

(15) Gao, Y. S., Hubbert, C. C., Lu, J., Lee, Y. S., Lee, J. Y., and Yao, T. P. (2007) Histone deacetylase 6 regulates growth factor-induced actin remodeling and endocytosis. *Mol. Cell. Biol. 27*, 8637−8647.

(16) Kalin, J. H., and Bergman, J. A. (2013) Development and Therapeutic Implications of Selective Histone Deacetylase 6 Inhibitors. *J. Med. Chem. 56*, 6297−6313.

(17) Butler, K. V., Kalin, J., Brochier, C., Vistoli, G., Langley, B., and Kozikowski, A. P. (2010) Rational Design and Simple Chemistry Yield a Superior, Neuroprotective HDAC6 Inhibitor, Tubastatin A. *J. Am. Chem. Soc. 132*, 10842−10846.

(18) Kalin, J. H., Butler, K. V., Akimova, T., Hancock, W. W., and Kozikowski, A. P. (2012) Second-Generation Histone Deacetylase 6 Inhibitors Enhance the Immunosuppressive Effects of Foxp3+ T-Regulatory Cells. *J. Med. Chem. 55*, 639−651.

(19) Bergman, J. A., Woan, K., Perez-Villarroel, P., Villagra, A., Sotomayor, E. M., and Kozikowski, A. P. (2012) Selective Histone Deacetylase 6 Inhibitors Bearing Substituted Urea Linkers Inhibit Melanoma Cell Growth. *J. Med. Chem. 55*, 9891−9899.

(20) Aditya, A., and Kodadek, T. (2012) Incorporation of Heterocycles into the Backbone of Peptoids to Generate Diverse Peptoid-Inspired One Bead One Compound Libraries. *ACS Comb. Sci. 14*, 164−169.

(21) Vannini, A., Volpari, C., Filocamo, G., Casavola, E. C., Brunetti, M., Renzoni, D., Chakravarty, P., Paolini, C., De Francesco, R., Gallinari, P., Steinkuhler, C., and Di Marco, S. (2004) Crystal structure of a eukaryotic zinc-dependent histone deacetylase, human HDAC8, complexed with a hydroxamic acid inhibitor. *Proc. Natl. Acad. Sci. U. S. A. 101*, 15064−15069.

(22) Waltregny, D., Glenisson, W., Tran, S. L., North, B. J., Verdin, E., Colige, A., and Castronovo, V. (2005) Histone deacetylase HDAC8 associates with smooth muscle alpha-actin and is essential for smooth muscle cell contractility. *FASEB J. 19*, 966−968.

(23) Lee, H., Sengupta, N., Villagra, A., Rezai-Zadeh, N., and Seto, E. (2006) Histone deacetylase 8 safeguards the human ever-shorter telomeres 1B (hEST1B) protein from ubiquitin-mediated degradation. *Mol. Cell. Biol. 26*, 5259−5269.

(24) Lee, H., Rezai-Zadeh, N., and Seto, E. (2004) Negative regulation of histone deacetylase 8 activity by cyclic AMP-dependent protein kinase A. *Mol. Cell. Biol. 24*, 765−773.

(25) Somoza, J. R., Skene, R. J., Katz, B. A., Mol, C., Ho, J. D., Jennings, A. J., Luong, C., Arvai, A., Buggy, J. J., Chi, E., Tang, J., Sang, B. C., Verner, E., Wynands, R., Leahy, E. M., Dougan, D. R., Snell, G., Navre, M., Knuth, M. W., Swanson, R. V., McRee, D. E., and Tari, L. W. (2004) Structural snapshots of human HDAC8 provide insights into the class I histone deacetylases. *Structure 12*, 1325−1334.

(26) Haberland, M., Montgomery, R. L., and Olson, E. N. (2009) The many roles of histone deacetylases in development and physiology: implications for disease and therapy. *Nat. Rev. Genet. 10*, 32−42.

(27) Huber, R. G., Margreiter, M. A., Fuchs, J. E., von Grafenstein, S., Tautermann, C. S., Liedl, K. R., and Fox, T. (2014) Heteroaromatic pi-stacking energy landscapes. *J. Chem. Inf. Model. 54*, 1371−1379.

(28) Bissantz, C., Kuhn, B., and Stahl, M. (2010) A Medicinal Chemist's Guide to Molecular Interactions. *J. Med. Chem. 53*, 5061−5084.

(29) He, C., Chen, J., An, L., Wang, Y., Shu, Z., and Yao, L. (2015) Carboxyl-peptide plane stacking is important for stabilization of buried E305 of Trichoderma reesei Cel5A. *J. Chem. Inf. Model. 55*, 104−113.

(30) De Vos, K. J., Grierson, A. J., Ackerley, S., and Miller, C. C. (2008) Role of axonal transport in neurodegenerative diseases. *Annu. Rev. Neurosci. 31*, 151−173.

(31) Balboni, G., Guerrini, R., Salvadori, S., Bianchi, C., Rizzi, D., Bryant, S. D., and Lazarus, L. H. (2002) Evaluation of the Dmt−Tic Pharmacophore: Conversion of a Potent δ-Opioid Receptor Antagonist into a Potent δ Agonist and Ligands with Mixed Properties. *J. Med. Chem. 45*, 713−720.

(32) TenBrink, R. E., Im, W. B., Sethy, V. H., Tang, A. H., and Carter, D. B. (1994) Antagonist, Partial Agonist, and Full Agonist Imidazo[1,5-a]quinoxaline Amides and Carbamates Acting through the GABAA/Benzodiazepine Receptor. *J. Med. Chem. 37*, 758−768.

(33) Choong, I. C., Lew, W., Lee, D., Pham, P., Burdett, M. T., Lam, J. W., Wiesmann, C., Luong, T. N., Fahr, B., DeLano, W. L., McDowell, R. S., Allen, D. A., Erlanson, D. A., Gordon, E. M., and O'Brien, T. (2002) Identification of Potent and Selective Small-Molecule Inhibitors of Caspase-3 through the Use of Extended Tethering and Structure-Based Drug Design. *J. Med. Chem. 45*, 5005−5022.

(34) Luckhurst, C. P. M; Springthorpe, B. (2004) Preparation of piperidine derivatives for use in the treatment of chemokine mediated disease states, Patent WO2004029041.

(35) Morris, G. M., Goodsell, D. S., Halliday, R. S., Huey, R., Hart, W. E., Belew, R. K., and Olson, A. J. (1998) Automated docking using a Lamarckian genetic algorithm and an empirical binding free energy function. *J. Comput. Chem. 19*, 1639−1662.